This manuscript has been submitted for publication in *Rapid Communications in Mass Spectrometry.* **This manuscript is under review and has yet to be accepted for publication. Subsequent versions of this manuscript may have slightly different content. If accepted, the final version of this manuscript will be available via the 'Peer-reviewed Publication DOI' link on the right-hand side of this webpage.**

Equilibrated gas and carbonate standard-derived paired clumped isotope (Δ_{47} and Δ_{48}) values on the absolute reference frame

Jamie K. Lucarelli[1], Hannah M. Carroll[1], Ben M. Elliott[1], Tyler B. Coplen[2], Robert A. Eagle[1], Aradhna Tripati[1]

[1]Department of Earth, Planetary, and Space Sciences, Department of Atmospheric and Oceanic Sciences, Institute of the Environment and Sustainability, Center for Diverse Leadership in Science, UCLA, Los Angeles, CA 90095 USA.

[2]US Geological Survey, 12201 Sunrise Valley Drive, Reston, VA, 20192, USA

Correspondence to: jklucarelli@gmail.com and atripati@g.ucla.edu

Equilibrated gas and carbonate standard-derived paired clumped isotope (Δ_{47} and Δ_{48}) values on the absolute reference frame

Rapid Communications in Mass Spectrometry

Jamie K. Lucarelli[1], Hannah M. Carroll[1], Ben M. Elliott[1], Tyler B. Coplen[2], Robert A. Eagle[1], Aradhna Tripati[1]

[1]Department of Earth, Planetary, and Space Sciences, Department of Atmospheric and Oceanic Sciences, Institute of the Environment and Sustainability, Center for Diverse Leadership in Science, UCLA, Los Angeles, CA 90095 USA.
[2]US Geological Survey, 12201 Sunrise Valley Drive, Reston, VA, 20192, USA
Correspondence to: jklucarelli@gmail.com and atripati@g.ucla.edu

Running Head: Robust Methods for Paired Carbonate Clumped Isotope Analysis (Δ_{47} and Δ_{48}) via IRMS

Rationale: Carbonate clumped isotope geochemistry has primarily focused on mass spectrometric determination of *m/z* 47 CO_2 for geothermometry, but theoretical calculations and recent experiments indicate paired analysis of the *m/z* 47 ($^{13}C^{18}O^{16}O$) and *m/z* 48 ($^{12}C^{18}O^{18}O$) isotopologues (referred to as Δ_{47} and Δ_{48}) can be used to study non-equilibrium isotope fractionations and refine temperature estimates. We utilize a multi-year and multi-instrument dataset to constrain Δ_{47} and Δ_{48} values for 27 samples, including standards and Devils Hole cave calcite, and study equilibrium Δ_{47}-Δ_{48}, Δ_{47}-temperature, and Δ_{48}-temperature relationships.
Methods: A total of 5,465 Δ_{47} and 3,400 Δ_{48} measurements of carbonates, and 183 Δ_{47} and 195 Δ_{48} measurements of gas standards from 2015-2021 from multiple mass spectrometers were used. We compare results to previously published findings.
Results: We report Δ_{47} and Δ_{48} values for 27 carbonates. We provide further experimental constraints on the equilibrium relationship between Δ_{47} and Δ_{48}. We report Δ_{47} and Δ_{48} relationships with temperature using a combination of theory and experimental regression-form acid digestion fractionation factors, $\Delta^*_{63\text{-}47}$ and $\Delta^*_{64\text{-}48}$.
Conclusions: This large dataset provides Δ_{48} values of carbonate standards for use in carbonate standard-based standardization. A robust Δ_{47}-Δ_{48} equilibrium regression was determined with data presented here and from previously published datasets. Regressions for Δ_{47} and Δ_{48} relationships with temperature are also presented.

1. INTRODUCTION

Equilibrium constants for internal isotope exchange reactions in carbonate minerals are directly related to their formation temperature.[1,2] This temperature dependence is the basis for carbonate clumped isotope thermometry, a tool for paleotemperature reconstruction in the geosciences. For minerals that form in isotopic equilibrium, the frequency with which rare, heavy isotopes in carbonate minerals are bonded to each other (instead of bonded to much more common light isotopes) relative to a stochastic (random) distribution is proportional to precipitation temperature.

There are multiple clumped isotopologues containing paired heavy isotopes in carbonate minerals that can potentially be used for geothermometry. The abundance of the dominant *m/z* 63 isotopologue ($^{13}C^{18}O^{16}O_2$) forms the basis of the most widely used thermometer. The acid digestion of minerals containing carbonate ion groups with *m/z* of 63 yields *m/z* 47 CO_2, which can then be measured by isotope ratio mass spectrometry.[1] Theory predicted that the lower abundance *m/z* 48 CO_2 isotopologue derived from acid digestion of *m/z* 64 ($^{12}C^{18}O_2{}^{16}O$) carbonate ion groups in equilibrium precipitates could be used for geothermometry [1,3–6] and this has recently been confirmed through experimentation.[7–10]

The abundance of the $^{13}C^{18}O^{16}O$ and $^{12}C^{18}O^{18}O$ isotopologues is denoted with Δ_{47} and Δ_{48} notation.[11] These are defined as:

$$\Delta_{47} = [(R47_{sample}/R47_{stochastic} - 1) \qquad \text{Equation 1}$$

$$\Delta_{48} = (R48_{sample}/R48_{stochastic} - 1) \qquad \text{Equation 2}$$

where Ri_{sample} is the measured ratio of i/44 CO_2 isotopologues in the sample, $Ri_{stochastic}$ is the ratio of i/44 CO_2 isotopologues that would be expected in a random distribution, and Δ_{47} and Δ_{48} values are typically multiplied by a factor of 1000 and given in permil (‰).[2,12] The most abundant *m/z* 48 CO_2 isotopologue ($^{12}C^{18}O^{18}O$) has two ^{18}O substitutions and is therefore in extremely low abundance at 4.1 ppm in air, which is an order of magnitude lower than *m/z* 47 isotopologues (45 ppm).[1] The minor *m/z* 48 CO_2 isotopologue ($^{13}C^{18}O^{17}O$) has an abundance of 16.7 ppb.[1]

The precise measurement of Δ_{47} was enabled by modification of the Thermo MAT 253, specially configured with *m/z* 47-49 Faraday cups and digestion and purification methods for carbonate minerals.[1,11] On this instrument, *m/z* 48 isotopologues were used only to screen for contaminants. Measurements of Δ_{48} have recently emerged as a tool for the study of equilibrium and kinetic isotope effects due to the use of 10^{13} Ω resistors for *m/z* 47-49 Faraday cups in the Thermo MAT 253 Plus[7–10], and secondary electron suppression in the Nu Perspective IS. These advances contribute to increased accuracy and precision for determination of Δ_{48} values, and paired Δ_{47} and Δ_{48} values on the absolute reference frame.

A unique attribute of carbonate clumped isotope thermometry based on Δ_{47} or Δ_{48} is that it does not depend on the bulk oxygen isotope composition ($\delta^{18}O$) of the water the carbonate precipitated from[1], unlike the more widely used oxygen isotope

thermometer[13]. Δ_{47} measurements have been used for the reconstruction of numerous paleo-environmental parameters, including but not limited to land[14] and ocean[5,15] paleotemperatures, paleoelevation[16,17], and dinosaur body temperature[18], while simultaneously estimating water $\delta^{18}O$. Previous research has shown that kinetic isotope effects observed in abiotic and biogenic carbonates, including speleothems[19,20] and coral[8,21–23], may affect the accuracy of Δ_{47}-based temperature reconstructions. However, the paired analysis of Δ_{47} and Δ_{48} has been shown by theory[2,4,5,24,25] and experimentation[7–10] to have a characteristic equilibrium relationship to temperature which may be used to identify and study kinetic effects in carbonates, if sufficiently accurate and precise measurements can be made.

Several studies have proposed the use of new methods to advance the consistency of measurements between laboratories and have improved the accuracy and precision of Δ_{47} determinations by mass spectrometry. Interlaboratory reproducibility of Δ_{47} values was advanced by using accurately determined carbonate standard values that are anchored to the absolute reference frame, using a reference frame constructed using primary gas standards, secondary carbonate standards, or a mixture of gas and carbonate standards, detailed by Dennis et al.[26], allowing for interlaboratory standardization. Recent work from Bernasconi et al.[27] has proposed nominal carbonate standard Δ_{47} values and the use of carbonate standards for standardization in the 90 ^{o}C reference frame. These advances form the foundation for assessing whether carbonate standardization can be used to yield Δ_{48} values, and paired Δ_{47} and Δ_{48} values, on the absolute reference frame that are intercomparable between instruments.

Here, we utilize large datasets collected over multiple years on multiple instruments for this purpose. Due to the low abundance of *m/z* 48 CO_2 isotopologues and potential for analytical error, the development of robust standard values is critical in ensuring accurate determination of unknown sample Δ_{48} values. Given the size of the dataset and the use of multiple instruments, we assessed if there were standardized methods of outlier analysis. In the literature, for outlier identification, one group of publications used outlier tests. Zaarur et al.[28] used a Peirce outlier test to identify and remove replicate Δ_{47}, $\delta^{18}O$, and $\delta^{13}C$ values that were statistical outliers, resulting in the exclusion of ~2% of data. They report this affected Δ_{47} in the third decimal place. Burgener et al.[29] used this same test to determine one sample Δ_{47} value was an outlier relative to the other samples in the dataset. Peral et al.[30] used Grubbs' outlier test to show that a Δ_{47} value for a foraminifera sample was an outlier when compared to the rest of their sample set. A second group of publications have used absolute deviations from mean values as cutoffs. Meckler et al.[31] excluded standard replicates with an offset greater than ± 0.03 ‰ from the mean value in each run. Upadhyay et al.[32] excluded replicates with an offset greater than ± 0.075 ‰ from the mean value. A third group of publications uses ancillary data. Tripati et al.[5] used Δ_{48} values of > 1 per mil (Δ_{48} excess) to be potentially indicative of contamination, and screened data if replicate level $\delta^{13}C$ or $\delta^{18}O$ values differed from the population mean by more than 3σ. Tripati et al.[33]

used Δ_{48} excess, and also used a Q-test (which identifies outliers at a 5σ level), for data quality assurance. Bernasconi et al.[27] worked with data that was provided by laboratories, based on each laboratory's own criteria for quality assurance to produce publication-grade results.

Here, we used both equilibrated gas and carbonate-based standardization to report the isotopic composition of 27 carbonates, including standards and 4 Devils Hole calcite samples[34,35], determined on different mass spectrometer configurations over multiple years. We use this data and theory to explore clumped isotope equilibrium relationships. We also report statistical methods for data processing of large datasets. We compared use of a 3σ and 5σ cutoff for outlier exclusion. We determine regression-form acid digestion fractionation factors for the phosphoric acid digestion of *m/z* 63 and *m/z* 64 CO_3^{2-} to *m/z* 47 and *m/z* 48 CO_2, respectively.

2. METHODS

2.1 Carbonates analyzed

In total, 27 different carbonates were analyzed for clumped and bulk isotope compositions on mass spectrometers in the Tripati Lab at University of California, Los Angeles. Table 1 contains a description of the mineralogy and origin of all carbonates, modified from Upadhyay et al.[32] These materials were chosen for analysis because many of them are standards used widely among clumped isotope laboratories, such as the ETH standards and Carrara Marble. Others are used commonly in a certain region or country, such as ISTB-1, TB-1, and TB-2, which are clumped isotope standards from the China University of Geosciences. Additionally, this suite of samples encompasses numerous carbonate types, including biogenic materials, and carbonates of different mineralogies. Some of the materials are presumed to have near equilibrium clumped isotope values, such as Devils Hole mammillary calcite, ETH-1, and ETH-2. Many also have a large number of analyses (n > 50) on one or multiple instruments that can be used to provide robust standard values for Δ_{47} and Δ_{48} measurements on the absolute reference frame.

2.2 Devils Hole calcite

We analyzed four Devils Hole (Amargosa Desert, Nevada) mammillary calcite samples from core DH-2 for paired Δ_{47} and Δ_{48} values, including DH-10 (172 ± 4 ka), DH-11 (163 ± 5 ka), DH-12 (57 ± 5 ka), and DH-13 (151 ± 4 ka)[34], that previously were measured for Δ_{47} in Tripati et al.[5] The samples were re-analyzed on Nu Perspective mass spectrometers. Devils Hole calcite is assumed to have precipitated near isotopic equilibrium due to an extremely slow precipitation rate (0.1-0.8 μm $year^{-1}$) in water with

a low calcite saturation index (0.16-0.21).[35,36] Devils Hole is thought to have had a stable temperature of 33.7 (±0.8) °C throughout the Holocene.[34–37]

2.3 Instrumentation

Standards and samples were analyzed on 3 mass spectrometers using 5 configurations (Table 2), including Nu Perspective-EG, Nu Perspective-1, Nu Perspective-1a, Nu-Perspective-2, and MAT 253. Nu Perspective-EG, Nu Perspective-1, and Nu Perspective-1a use the same mass spectrometer with differences in the acid digestion system, ion beam intensity, and integration time. Nu Perspective-EG is the only configuration that analyzed equilibrated gases. On both the MAT 253 and Nu Perspective mass spectrometers, the detectors for *m/z* 44 through 46 are registered through 3×10^8, 3×10^{10}, and 10^{11} Ω resistors, respectively, while detectors for *m/z* 47 through 49 are registered with 10^{12} Ω resistors.

The most notable difference between Nu Instruments Perspective and the more widely used older generation Thermo Fisher MAT 253 is the implementation in the former of electrostatic analyzers (ESAs) before the *m/z* 47-49 detectors. These ESAs consist of two curved plates with a voltage difference placed directly in front of each of the Faraday collectors. The addition of the ESAs as well as ion lenses following the magnetic sector of the flight tube removes secondary ion and electron signals from the mass detection. This removal results in a drastic reduction in the interfering signals on all masses (*m/z* 44-49) during operation, producing flatter and more stable baselines, relative to the older MAT 253 (Figure S1). In addition, the lowered interference from secondary electrons in the Nu Perspectives results in greater intensities and lowered noise in the signals from the higher masses, especially *m/z* 48 and 49. This advancement has contributed to a Δ_{47} non-linearity slope for the Nu Perspective (median slope observed was -0.00005) that ranges from one to two orders of magnitude less than the MAT 253 (median slope observed was -0.007), and a Δ_{48} non-linearity slope for the Nu Perspective (median slope observed was -0.004) that is an order of magnitude less than the MAT 253 (median slope observed was -0.013).

Nu Perspective-EG, Nu Perspective-1, Nu Perspective-1a, and MAT 253 use an in-house constructed autosampler that is similar to the setup detailed in Passey et al.[38] The configuration uses a stainless steel Costech Zero Blank autosampler and a 105 % phosphoric acid bath that digests calcium carbonate samples at 90 °C. The sample gas passes through cryogenic purification traps that use dry ice-cooled ethanol and liquid nitrogen to remove contaminant gases that have low vapor pressure, mostly consisting of water vapor. The CO_2 gas then passes through elemental silver wool (Sigma-Aldrich) to remove sulfur compounds, followed by a gas chromatograph (GC) column with helium carrier gas that contains Porapak Type-Q™ 50/80 mesh column packing material to remove organic compounds. The GC column is maintained at a constant

temperature of -20 °C during sample purification. Large samples weighing 4-7 mg are analyzed on the MAT 253 in bellows with a total integration time of 720 s. Small samples weighing 0.5 mg are analyzed in bellows on Nu Perspective-EG and Nu Perspective-1 mass spectrometer (they use the same mass spectrometer) with 3 blocks of 20 cycles, with a total integration time of 1600 s. Nu Perspective-1a also uses the same mass spectrometer, but the sample and working gas volumes are depleted in microvolume mode at precisely matched rates, with *m/z* 44 ranging from 80-30 nA during sample acquisition, with an integration time of 1200 s. The sample preparation system is operated by custom software in Labview that controls the sampler, GC column, cryogenic dewar lifters, and valves. The Labview software is integrated with the Perspective Stable Gas Control software interface that controls the Nu Perspective mass spectrometer.

Nu Perspective-2 uses a Nu Carb Sample Digestion System instead of a common acid bath, where 0.5 mg of calcium carbonate is reacted at 70 °C in individual glass vials with 105 wt% phosphoric acid. The sample gas is cryogenically purified in liquid nitrogen-cooled tubes called coldfingers before passing through a relatively short GC column packed with Porapak Type-Q™ 50/80 and silver wool. This instrument operates under vacuum pressure and does not use a carrier gas. The sample and working gas volumes are matched precisely during depletion into the mass spectrometer, with *m/z* 44 ranging from 80-30 nA. Sample data is analyzed in 3 blocks of 20 cycles, with each cycle integrating for 20 s, for a total integration time of 1200 s.

2.4 Equilibrated gas standards

We analyzed 195 equilibrated gas standards on a Nu Instruments Perspective mass spectrometer, here called Nu Perspective-EG. We utilized two gases with differing bulk isotope values, with a ~60 ‰ difference in δ_{47} values, prepared using standard procedures[1,26]. The heavy isotope depleted δ_{47} gas is from an Airgas CO_2 gas cylinder and was equilibrated with 5-10 mL of 25 °C deionized (DI) water. The heavy isotope enriched δ_{47} gas is produced by phosphoric acid digestion of a Carrara Marble carbonate standard. The resulting carbon dioxide was equilibrated with evaporated DI water held at 25 °C. Aliquots of the two 25 °C gases are re-equilibrated at 1000 °C by heating the gases in quartz tubes inside a muffle furnace for >1 hour, and then flash cooled, to produce gases with near stochastic Δ_{47} values.

2.5 Data processing and normalization

Raw data files from all instrument configurations were transferred into Easotope[39] (64-bit version from release 20201231), where corrections and final Δ_{47} and Δ_{48} values for replicates were calculated. All data used the IUPAC parameter set.[40,41] Δ_{47} and Δ_{48}

data from Nu Perspective-EG is reported on the Carbon Dioxide Equilibrium Scale (CDES 90; Dennis et al.[26]), meaning it was normalized to CO_2 equilibrated at 25 °C and 1000 °C at an acid digestion temperature of 90 °C. Δ_{47} data from Nu Perspective-1, Nu Perspective-2, and MAT 253 is reported on the InterCarb-Carbon Dioxide Equilibrium Scale (I-CDES; Bernasconi et al.[27]), meaning it was normalized to carbonate standards including ETH-1, ETH-2, and ETH-3 at an acid digestion temperature of 90 °C. Note that the I-CDES and CDES 90 reference frames should be equivalent if properly standardized. Δ_{48} data for Nu Perspective-1, Nu Perspective-2, and MAT 253 are reported on the CDES 90 scale, normalized to carbonate standards including ETH-1, ETH-2, and ETH-3 at an acid digestion temperature of 90 °C. Since it currently is convention to describe Δ_{48} values digested at 90 °C as CDES 90 whether they are normalized to equilibrated CO_2 or carbonate standards, we want to note again that the only instrument here that used equilibrated CO_2 normalization was Nu Perspective-EG, while the others use exclusively carbonate standard based normalization.

Figure 1 contains a flow chart detailing the standards used in data normalization for each instrument configuration. Methods detailed in Dennis et al. (2011) were used to normalize data to the CDES 90 and I-CDES reference frames, including a nonlinearity correction and transfer function (Figures 1, 2). We do not perform pressure baseline corrections; however, a background correction is performed for all masses (*m/z* 44-49) on all instruments before any further data normalization. The background is measured (in amps on the Nu Perspective instruments; mV on the MAT 253) at the start of an analysis and is subtracted from the measurement. For the nonlinearity slope correction, a slope was determined over a 10-day moving average for the regression lines between $\delta_{47\ raw}$ and $\Delta_{47\ raw}$, and $\delta_{48\ raw}$ and $\Delta_{48\ raw}$ values for CO_2 gas standards equilibrated at 25 °C and 1000 °C or ETH-1 and ETH-2 (Figure 2A, B, E, F). Nonlinearity slope corrections are applied to all analyses using equations 3 and 4:

$$\Delta_{47\ sc} = \Delta_{47\ raw} - (m_{47} \times \delta_{47\ raw}) \qquad \text{Equation 3}$$

$$\Delta_{48\ sc} = \Delta_{48\ raw} - (m_{48} \times \delta_{48\ raw}) \qquad \text{Equation 4}$$

where $\Delta_{47\ sc}$ and $\Delta_{48\ sc}$ values are the nonlinearity slope-corrected values, and m_{47} and m_{48} are the regression slopes, with nomenclature adapted from Fiebig et al.[7] For the transfer function, the 10-day moving average slope and intercept was determined for the linear relationship between either theoretically calculated Δ_{47} values for 25 °C and 1000 °C, 0.925 ‰[42] and 0.027 ‰[26], respectively, or carbonate standard values, and $\Delta_{47\ sc}$ values (Fig. 2C, D, G, H). Where carbonate standards where used, Δ_{47} values determined in Bernasconi et al.[27] of 0.2052 ‰, 0.2085 ‰, and 0.6132 ‰ were used as standard values for ETH-1, ETH-2, and ETH-3, respectively. For Nu Perspective-2, the additional standards Carmel Chalk and Veinstrom were used, with Δ_{47} values of 0.674

‰ and 0.715 ‰, respectively. Before Carmel Chalk and Veinstrom were used in data normalization, their long-term average values were determined on Nu Perspective-1 and MAT 253. For Δ_{48}, the 10-day moving average slope and intercept was determined for the linear relationship between either theoretically calculated Δ_{48} values for 25 °C and 1000 °C of 0.345 ‰[42] and 0.000 ‰[7], respectively, or carbonate standards, and $\Delta_{48\,sc}$. Where carbonate standards were used, the Δ_{48} values determined on Nu Perspective-EG for ETH-1, ETH-2, ETH-3, and Veinstrom (Table 3) were used for standard values. The transfer function (TF) slope and intercept from these regressions were used to create transfer functions, which are applied to all $\Delta_{47\,sc}$ and $\Delta_{48\,sc}$ values, and yields the fully corrected values Δ_{47} and Δ_{48} values using equations 5 and 6:

$$\Delta_{47\,\text{I-CDES; CDES 90}} = \Delta_{47\,sc} \times \text{TF slope} + \text{TF intercept} \qquad \text{Equation 5}$$

$$\Delta_{48\,\text{CDES 90}} = \Delta_{48\,sc} \times \text{TF slope} + \text{TF intercept} \qquad \text{Equation 6}$$

where Δ_{47} and Δ_{48} values are the fully corrected values in the I-CDES or CDES 90 reference frame, $\Delta_{47\,sc}$ and $\Delta_{48\,sc}$ values are the slope corrected values from equations 3 and 4, TF slope is the transfer function slope, and TF intercept is the transfer function intercept.

2.6 Use of statistical methods for robust determination of Δ_{47} and Δ_{48} values

We report a large historical dataset where many standards have >100 replicates. To streamline data analyses and ensure all replicate data was handled identically, we developed an R script that automated outlier identification, calculation of sample mean values (replicate pool average), error (replicate pool error reported as ±1 SE), and data statistics. In the Appendix we provide a detailed description of this method for replicate-level outlier identification and data pooling from multiple instruments. The R script is publicly available for review at https://github.com/Tripati-Lab/Lucarelli-et-al. This method is particularly useful for datasets with a large number of replicates where determining outliers manually can be time intensive; it also helps reduce potential human bias. We do not recommend this method for samples with less than 12 replicates, as this was the smallest number of replicates we successfully tested the method on. In short, a density function was determined for replicate level data for each sample on every instrumental configuration after an initial removal of very large outliers (i.e., Δ_{47} or Δ_{48} values of <-0.5) (Figure 3B). A 3σ or 5σ (3 standard deviations from the mean or 5 standard deviations from the mean) cut was then made for each density function (Figure 3C). Then, the final replicate pool for each sample was used to determine the average Δ_{47}, Δ_{48}, $\delta^{18}O$, and $\delta^{13}C$ values, SE, and normality of the data distribution. We note the error reported here

may not fully account for all error associated with transferring raw data into the final Δ_{47} values, described as "allogenic" errors by Daëron (2021). These errors may play a larger role for Δ_{48} given larger measurement uncertainties.

For data pooling between instrumental configurations, the Δ_{47} and Δ_{48} replicate distributions for standards and samples run on multiple instrument configurations (consistency standards) were directly compared. If no statistically significant differences were observed for standard and consistency standard values between configurations, replicates were pooled to calculate a combined average. Δ_{48} replicate values from the MAT 253 were not pooled with replicate values from the Nu Perspective instruments.

2.7 Calculation of Δ_{47}-T and Δ_{48}-T equilibrium relationships using regression-form acid fractionation factors

Temperature-dependent Δ_{47} and Δ_{48} equilibrium relationships were calculated using equilibrium calcite Δ_{63} and Δ_{64} values predicted by theory from Hill et al.[4] and Tripati et al.[5], combined with regression-form acid fractionation factors (AFFs), $\Delta^*_{63\text{-}47}$ and $\Delta^*_{64\text{-}48}$ using equations 7 and 8.

$$\Delta_{47\ \text{I-CDES EQ}} = \Delta_{63} + \Delta^*_{63\text{-}47} \qquad \text{Equation 7}$$

$$\Delta_{48\ \text{CDES 90 EQ}} = \Delta_{64} + \Delta^*_{64\text{-}48} \qquad \text{Equation 8}$$

Model calculations from Guo et al.[3] predicted that AFFs for when calcite mineral is digested in phosphoric acid, $\Delta^*_{63\text{-}47}$ and $\Delta^*_{64\text{-}48}$, should depend on the Δ_{63} and Δ_{64} values of the reactant carbonate, respectively. Thus, regression form AFFs were determined by taking the theoretical Δ_{63} and Δ_{64} values at two temperatures, 600 ^{o}C and 33.7 ^{o}C, and then subtracting the experimental Δ_{47} and Δ_{48} values for samples with known precipitation temperatures at 600 ^{o}C and 33.7 ^{o}C. Then, a linear regression was made between the $\Delta^*_{63\text{-}47}$ and $\Delta^*_{64\text{-}48}$ values for 600 ^{o}C and 33.7 ^{o}C and the corresponding theoretically predicted Δ_{63} and Δ_{64} values for 600 ^{o}C and 33.7 ^{o}C (Hill et al.[4]; Tripati et al.[5]). The experimental Δ_{47} and Δ_{48} values used for 600 ^{o}C were the pooled replicate values for ETH-1 and ETH-2 (Bernasconi et al.[43]), and the values used for 33.7 ^{o}C were from pooled replicate values for Devils Hole calcite (Coplen,[35]). Further details of this calculation are in Appendix Section A.2.

3. RESULTS

3.1 Use of statistical methods for robust determination of Δ_{47} and Δ_{48} values

We find there was a negligible difference in the number of replicates removed when a 3σ versus 5σ cutoff was used for outliers due to narrow peak widths (Figure S2, Table S1). To further ensure the robustness of this method, we compared our final Δ_{47} values to Upadayay et al.[32] which presented a subset of the data reported here using other methods for outlier removal and data processing (Table S2). The datasets are in good agreement, with an average offset of 0.011 ‰, despite the Δ_{47} data from their study being standardized differently than the data here, and then being transferred into the I-CDES reference frame using an equation from Appendix A in Bernasconi et al.[27].

3.2 Instrumental configuration comparison

We found no evidence of statistically significant differences in the final Δ_{47} or Δ_{48} values of samples analyzed on multiple configurations (Figure S3; Table S3, S4). However, Δ_{48} data from the MAT 253 was not pooled with Nu Perspective-1 and Nu Perspective-2 data because offsets were observed in Δ_{48} values for the standards ETH-1 and ETH-2 that did not exist in Nu Perspective-1 and Nu Perspective-2 (Table 4). The older generation MAT 253 does not use secondary electron suppression, and therefore, does not yield as precise Δ_{48} data as the Nu Perspective instruments, which do use secondary electron suppression. Additionally, we have not combined data produced using equilibrated gas-based standardization with data produced using carbonate-based standardization.

3.3 Δ_{47} and Δ_{48} results

Δ_{47} and Δ_{48} values were determined for 7 standards using 25 ºC and 1000 ºC equilibrated gas-based standardization, with a total of 324 Δ_{47} and 363 Δ_{48} replicate analyses performed from May 2015-June 2017 (Table 3). Additionally, Δ_{47} values were determined for 27 standards and samples (5,141 replicate analyses), and Δ_{48} values (3,037 replicate analyses) for 24 standards and samples using carbonate-based standardization, performed from April 2015-March 2021 (Table 4). All Δ_{47} sample replicate-level data were normally distributed, with the exception of ETH-3 analyzed on MAT 253 (Table S5). All Δ_{48} replicate-level data were normally distributed (Table S6).

We also present Δ_{48} data produced on the older generation MAT 253 mass spectrometer (Table 4). Due to higher error, lower precision, and offsets in ETH-1 and ETH-2 values, we did not pool Δ_{48} replicate data produced on the MAT 253 with the data produced on the Nu instruments. However, Δ_{48} data from the MAT 253 is included here due to the large amount of clumped isotope data produced on this instrument going back to 2014, given comments from J. Eiler (pers. comm.) indicating these instruments may produce usable Δ_{48} data. We sought to test as to whether this instrument, with sufficient replication and quality control, could produce reproducible Δ_{48}

values. We observed that the MAT 253 produced similar sample average values for the majority of samples (Table 4; Figure S3), with larger SE than the Nu Perspective instruments, as expected. Thus, it may be worth mining past MAT 253 datasets to examine Δ_{48} depending on the reproducibility of measurements, although newer generation instrumentation is preferable for the measurement of Δ_{48} values.

3.3.1 Experimentally determined Δ_{47}-Δ_{48} regression

The polynomial described by Equation 9 ($r^2 = 0.97$) was fit through experimentally determined Δ_{47} and Δ_{48} values for 20 samples, including standards and Devils Hole calcite (Figure 4A).

Equation 9

$$\Delta_{48\ \mathrm{CDES\ 90}} = (0.1179 \pm 0.0266) - (0.0398 \pm 0.1332)\Delta_{47\ \mathrm{I\text{-}CDES}} + (0.4407 \pm 0.1490)\Delta_{47\ \mathrm{I\text{-}CDES}}^2$$

All Δ_{47} and Δ_{48} values used to calculate this regression can be found in Table 4. Of the 21 total samples in Figure 4, all lie within 1 SE of the 95 % confidence interval of the regression, with the exception of Merck, Carmel Chalk, and 47407 Coral. 47407 Coral was the only sample not included in the regression due to its apparent offset from equilibrium.

3.4 Calculated Δ_{47}-T, Δ_{48}-T, and Δ_{47}-Δ_{48} regressions using regression-form AFFs

The calculated Δ_{47} and Δ_{48} equilibrium values for 0-1000 ^{o}C are in Table 5. These values were calculated using theoretical equilibrium Δ_{63} and Δ_{64} values for calcite (Hill et al.[4];Tripati et al.[5]) and regression-form AFFs determined here. The equilibrium Δ_{47} and Δ_{48} relationship (Figure 4A) is represented by equation 10.

Equation 10

$$\Delta_{48\ \mathrm{CDES\ 90\ EQ}} = 0.1123 + 0.01971\ \Delta_{47\ \mathrm{I\text{-}CDES\ EQ}} + 0.364(\Delta_{47\ \mathrm{I\text{-}CDES\ EQ}})^2$$

The temperature-dependent equilibrium relationships are described by equations 11 and 12,

Equation 11

$$\Delta_{47\ \mathrm{I\text{-}CDES\ EQ}} = [0.6646 \pm (0.0009)] - [0.0032 \pm (3.033 \times 10^{-5})]T + [(1.012 \times 10^{-5}) \pm$$

$(2.449 \times 10^{-7})]T^2 - [(1.559 \times 10^{-8}) \pm (6.717 \times 10^{-10})]T^3 + [(9.251 \times 10^{-12}) \pm (5.802 \times 10^{-13})]T^4$

Equation 12

$\Delta_{48\ \mathrm{CDES\ 90\ EQ}} = [0.2842 \pm (0.0009)] - [0.0014 \pm (3.048 \times 10^{-5})]T + [(5.741 \times 10^{-6}) \pm (2.437 \times 10^{-7})]T^2 - [(1.017 \times 10^{-8}) \pm (6.749 \times 10^{-10})]T^3 + [(6.570 \times 10^{-12}) \pm (5.830 \times 10^{-13})]T^4$

where temperature is in Celsius.

The regression form AFFs are represented by equations 13 and 14,

$\Delta^*_{63\text{-}47} = 0.0190 \times \Delta_{47\ \mathrm{I\text{-}CDES}} + 0.1842$ Equation 13

$\Delta^*_{64\text{-}48} = 0.0077 \times \Delta_{48\ \mathrm{CDES\ 90}} + 0.1290$ Equation 14

where $\Delta^*_{63\text{-}47}$ and $\Delta^*_{64\text{-}48}$ are the AFFs. These values can be used to estimate calcite mineral Δ_{63} and Δ_{64} values via equations 7 and 8 for comparison the theory. The use of a regression form AFF is more important for Δ_{47} than Δ_{48}, as there is a ~0.009 ‰ difference in $\Delta^*_{63\text{-}47}$ from 0-600 ^{o}C for Δ_{47}, while there is only a ~0.001 ‰ difference in $\Delta^*_{64\text{-}48}$ over the same temperature range (Table 5).

4. DISCUSSION

4.1 Comparison of Δ_{47} and Δ_{48} values determined with equilibrated gas-based standardization

Since Δ_{48} is a relatively new proxy, the development of robust standard values is of the utmost importance to ensure intra- and inter-laboratory reproducibility. To establish carbonate standard Δ_{48} values that can be used in data normalization for unknown samples, Δ_{48} values for carbonate standards must first be determined relative to equilibrated gases. We have compared our Δ_{47} and Δ_{48} values for carbonate standards determined using equilibrated gas-based standardization to other recently published datasets with paired clumped isotope values for ETH standards, including Fiebig et al.[7], Bajnai et al.[8], and Swart et al.[9] (Figure 5, Table 3). There is good interlaboratory agreement for Δ_{47} values, with a range of 0.002 ‰ to 0.012 ‰ for Δ_{47} offsets for replicated samples. The Δ_{47} error, reported as 1 SE, was similar (0.001 ‰ to 0.006 ‰) for all studies. When the Δ_{47} values for carbonate standards determined in these studies were compared to the multi-laboratory study from Bernasconi et al.[27]

which determined nominal Δ_{47} values for carbonate standards, there was similar agreement between laboratories, with offsets from 0.000 ‰ to 0.012 ‰ for replicated samples (Table 3). The interlaboratory Δ_{48} offsets were larger, with a range of 0.009 ‰ to 0.038 ‰ for replicated samples, although the majority of replicated samples were with within 1 SE of eachother (Table 3, Figure 5). The Δ_{48} error reported in Bajnai et al.[8] of 0.004 ‰ to 0.005 ‰ was lower than that for the other studies which have error ranging from 0.007 ‰ to 0.014 ‰, possibly from more replication, larger sample size (10 mg compared to 0.5 mg in this study), and longer mass spectrometric integration times than what was used here.

The use of equilibrated gases for standardization has been shown to be a potential source of error and interlaboratory offsets since the sample undergoes acid digestion and the gas standard does not, different laboratories use different setups to produce gas standards, and fractionations may occur from quenching during the production of heated gas standards[43]. However, interlaboratory Δ_{47} offsets up to 0.024 ‰ in Bernsconi et al.[27] were determined to be the result of random error which may be amplified during data normalization. The range in Δ_{47} offsets observed here are smaller than what was observed in Bernsconi et al.[27], likely from overall high replication. Additionally, we observed an average interlaboratory Δ_{48} offset of 0.018 ‰ (taken as the average of the absolute value of offsets of replicated samples in Table 3). These offsets are likely also from random error, considering that the *m/z* 48 isotopologue is an order of magnitude lower in abundance than the m/z 47 isotopologue[1], and this offset is still within the range of observed interlaboratory Δ_{47} offsets.

4.2 Carbonate based standardization for Δ_{47}-Δ_{48} measurements

Previously, important contributions have demonstrated that carbonate standard-based standardization that uses readily available materials can produce robust Δ_{47} values and yield interlaboratory discrepancies that are consistent with analytical uncertainties[27,31,43]. We applied this approach, using ETH-1, ETH-2, and ETH-3 as carbonate standards on multiple instruments in our laboratory for the paired analysis of Δ_{47}-Δ_{48}. The combined instrument average from this study (Table 4) and Bernsconi et al.[27] had excellent agreement between ETH standard Δ_{47} values, with offsets of 0.001, 0.002, 0.004, and 0.005 for ETH-1, ETH-2, ETH-3, and ETH-4 (used as an unknown), respectively. This is likely because the nominal Δ_{47} values determined in Bernasconi et al.[27] for ETH standards were used here in transfer functions for data normalization, adding supporting evidence for the importance of laboratories using common standard values to yield reproducible results. Similarly, carbonate standard-based standardization yielded reproducible Δ_{48} results (Figure 6) across the two Nu Perspective mass spectrometer configurations presented in Table 4. The Δ_{48} offsets for the 3 standards treated as unknowns (consistency standards), Carrara Marble, CM Tile, and ETH-4, that

were replicated on Nu Perspective-1 and Nu Perspective-2, ranged from 0.004 ‰ to 0.013 ‰. These offsets were reduced compared to interlaboratory Δ_{48} offsets observed for ETH standard values and Carrara Marble determined using equilibrated gas-based standardization (average: 0.018 ‰; minimum: 0.008 ‰; maximum: 0.038 ‰). Further, carbonate standard based standardization was successfully used by Bajnai et al.[44] for determining Δ_{48} values for Devils Hole cave calcite. There is currently no agreed upon Δ_{48} values for carbonate standards, thus, for laboratories that choose to employ carbonate-based standardization for Δ_{48} data and do not have in-house determined standard Δ_{48} values, the use of Δ_{48} values determined here for ETH-1 (0.132 ‰; n = 464), ETH-2 (0.132 ‰, n = 439), and ETH-3 (0.247 ‰; n = 236) may be used in carbonate-based standardization. Additional Δ_{48} values for materials that are widely used and may potentially be used as standards, such as Carrara Marble (n = 319), IAEA-C1 (n = 49), and IAEA-C2 (n = 59) are also in Table 4. Consistent with Daëron[45] and Kocken et al.[46], we recommend a 50:50 sample to standard ratio, which was what was utilized here.

4.3 Experimental Δ_{47}-Δ_{48} equilibrium regression using samples and standards

We determined an experimental Δ_{47}-Δ_{48} regression (equation 9) for 20 carbonate standards and samples (combined average values in Table 4). To have a constraint as to whether the materials included in the regression achieved quasi-equilibrium clumped isotope values, we compared the experimental regression to our equilibrium regression based on calcite mineral equilibrium theory[4,5] for Δ_{63}-Δ_{64} (Figure 4A). The theoretical regression for Δ_{63}-Δ_{64} equilibrium was transferred into Δ_{47}-Δ_{48} space with an experimentally determined regression-form AFF (see Methods 2.7). The materials used to determine the regression-form AFF to transfer theoretical Δ_{63}-Δ_{64} equilibrium values into Δ_{47}-Δ_{48} equilibrium values were the extremely slow growing calcite from Devils Hole and pooled values for ETH-1 and ETH-2. These materials have well-constrained precipitation temperatures and are believed to have achieved quasi-equilibrium clumped isotope values[35,43,44]. When the experimental regression using 20 carbonates was compared to the theoretical/experimental AFF regression, they were found to be statistically indistinguishable (P = 0.39; F = 1.03; Table S7). This supports the assumption that the materials used in the experimental regression have achieved quasi-equilibrium clumped isotope values.

Of the materials used in the regression, all lie within 1 SE of the 95 % confidence interval of the regression, with the exception of Merck, Carmel Chalk, and 47407 Coral. The 47407 Coral was the only sample for which we determined a Δ_{48} value that was not included in the regression. The possibility that Merck, an ultra-pure synthetic calcite, and Carmel Chalk, a natural calcite chalk, are exhibiting subtle clumped isotope disequilibrium cannot be excluded. However, both Merck and Carmel Chalk deviated

from the equilibrium regressions by <1 SD and therefore were included in the experimental regression, while 47407 Coral deviated from the regressions by >1 SD. 47407 Coral is a deep-sea coral of the genus *Desmophyllum* with an estimated growth temperature of 4.2 °C.[21] Guo et al.[24] used model estimates to predict a negative correlation between Δ_{47} and Δ_{48} values for cold-water corals, with kinetic effects causing enrichments in Δ_{47} values and depletions in Δ_{48} values. We determined that the 47407 Coral exhibits an enrichment of 0.030 ‰ in Δ_{47} and depletion of -0.018 ‰ in Δ_{48} by defining nominal equilibrium as the regression through the remaining carbonates, and the offsets were determined by using a kinetic slope for CO_2 absorption in corals of -0.6[8,24]. Bajnai et al.[8] also measured Δ_{47} and Δ_{48} values for a coral of the same genus (*Desmophyllum*) and a brachiopod (*Magellania venosa*) and observed similar enrichments in Δ_{47} (0.038 ‰ to 0.069 ‰) and depletions in Δ_{48} (-0.0004 ‰ to -0.095 ‰). Additionally, modeling from Guo et al.[24] and Bajnai et al.[8] predicts deviations from equilibrium of a similar magnitude.

4.4 Constraining equilibrium Δ_{47}-Δ_{48}

The equilibrium Δ_{47}-Δ_{48} relationship is of recent interest due to the potential for use to identify kinetic effects in biotic and abiogenic samples that are or could be used for paleotemperature reconstructions. As mentioned above, a recent study[8] used a kinetic slope calculated relative to a proposed equilibrium Δ_{47}-Δ_{48} regression to recover temperature signals in kinetically controlled samples. To further develop the use of Δ_{47}-Δ_{48} equilibrium as a proxy to constrain kinetic effects, the Δ_{47}-Δ_{48} equilibrium relationship must be well constrained. Thus, we compared the experimentally determined Δ_{47}-Δ_{48} regressions for quasi-equilibrium materials determined here (Equation 9) to those from Swart et al.[9] and Fiebig et al.[10] using a sum-of-squares F test (Table S7). This compares the fit of a regression through all datasets to the fit of individual regressions for each dataset, and tests whether the datasets differ sufficiently from each other to warrant separate regressions. The dataset from Swart et al.[9] contains 7 inorganic precipitations in 5 °C increments from 5 °C to 65 °C and carbonate standards ETH-1, ETH-2, ETH-3, and ETH-4. The dataset from Fiebig et al.[10] includes 16 carbonates, some of which are combined into averages, yielding 10 samples that are used for comparison here, including lake calcite, Devils Hole calcite, inorganic calcite precipitations, and calcite equilibrated at high temperatures, with crystallization temperatures for all samples ranging from 8 °C to 1100 °C. We found no evidence of statistically significant differences between the individual regressions ($P = 0.86$; $F = 0.43$; Table S7), and we therefore produced a combined regression (Figure 4B), described by equation 15, which is composed of 41 samples that are believed to have achieved quasi-equilibrium clumped isotope values.

Equation 15

$$\Delta_{48\ CDES\ 90} = (0.1132 \pm 0.010) + (0.008 \pm 0.055)\ \Delta_{47\ CDES\ 90} + (0.3692 \pm 0.065)\ \Delta_{47\ CDES\ 90}^2$$

Of the 41 materials used in the combined regression, 35 are within 1 SE of the 95 % confidence interval. The samples outside of the confidence interval include Carmel Chalk, ETH-4, and Merck from this study; ETH-2 and ETH-4 from Swart et al.[9]; and a cave lake calcite sample from Fiebig et al.[10]. It is unlikely that ETH-2 is exhibiting kinetic effects since it has an equilibration temperature of 600 °C[43], and has near stochastic isotopic values[47].The cave lake calcite sample from Fiebig et al.[10] is from Laghetto Basso, Italy with a precipitation temperature of 7.9 ± 0.2 °C. Fiebig et al[10] and Daëron et al.[48] argued that this sample precipitated close to equilibrium due to long residence times of water in the lake, low calcite saturation index (< 0.3), slow precipitation rate (0.3 μm/yr), and consistent δ^{18}O values for contemporaneously deposited calcite layers. It cannot be ruled out that ETH-4, the same commercially available calcite as ETH-2 but unheated[43], exhibits subtle kinetic effects. The ETH-4 sample from this study is much closer to the equilibrium regression than the ETH-4 sample from Swart et al.[9], mostly due to offsets in the Δ_{48} value (0.030 ‰) between the studies, which is larger than the offset for Δ_{47} (0.014 ‰). Both the Δ_{47} and Δ_{48} offsets between the studies are >2 SE but <1 SD, and within the threshold of observed scatter from random error[27], therefore, the difference in ETH-4 values between this study and Swart et al.[9] may be reflection of different standardization methods (carbonate-based standardization used here and equilibrated gas-based standardization in Swart et al.[9]) and measurement uncertainty. As discussed above in Section 4.3, it also cannot be ruled out that Carmel Chalk from this study exhibits subtle kinetic effects. However, the scatter for all samples and standards around the equilibrium line are well within what is expected from random error[27]. Further, the lack of statistical differences (P = 0.71; F = 0.46; Table S7) between the combined experimental regression and the theoretically based regression (equation 10) is evidence that equation 15 is a robust experimental representation of Δ_{47}-Δ_{48} equilibrium and can be used to constrain unknown sample kinetic biases.

4.5 Constraining equilibrium Δ_{47}-*T and* Δ_{48}-T

To date, four groups have published relationships for both Δ_{47}-*T* and Δ_{48}-*T*. The regressions from Swart et al.[9] and Fiebig et al.[10] are based on experimentally constrained values (as discussed in Section 4.4), while the regressions from this study and Bajnai et al.[8] are based on a combination of calcite mineral Δ_{63}-Δ_{64} equilibrium theory and experimental AFFs (see Methods 2.7). The Δ_{47}-*T* and Δ_{48}-*T* regressions from Bajnai et al.[8] was calculated for 0-40 °C, while the experimentally based regressions from Swart et al.[9] are for 0-65 °C. In this study we calculated Δ_{47}-*T* and Δ_{48}-*T* values

from 0-1000 °C, and Fiebig et al.[10] has experimentally constrained values up to 1100 °C. Due to the regressions from this study and Bajnai et al.[8] being theoretically based and therefore difficult to accurately provide an error calculation, we were unable to perform the same type of statistical analysis that compares the regressions, as we did for the experimental Δ_{47}-Δ_{48} regressions. Instead, we have compared the absolute difference between the regressions at 0 °C and 600 °C and compared this difference to measurement error observed in standards replicated between the laboratories. We used this metric to determine if it was appropriate to determine a combined regression. For Δ_{47}-T, the largest difference at 0 °C was 0.007 ‰ between this study and Bajnai et al.[8]. At 600 °C, an offset of 0.001 ‰ was calculated between this study and Fiebig et al.[10]. For Δ_{48}-T, the largest difference at 0 °C was 0.014 ‰ between this study and Bajnai et al.[8]. At 600 °C, an offset of 0.006 ‰ was calculated between this study and Fiebig et al.[10]. These offsets are well within the bounds of what we observed when comparing differences between ETH standard Δ_{47} and Δ_{48} values between laboratories (Section 4.1, Figure 5). This is a good metric for interlaboratory expected analytical error due to large numbers of replicates of ETH standards in all groups. The offsets are also within the bounds expected from random error in Δ_{47} measurements[27]. Therefore, we determined combined regressions for Δ_{47}-T and Δ_{48}-T (Figure 7), including this study, Bajnai et al.[8], Swart et al.[9], and Fiebig et al.[10], represented by equations 16 and 17

Equation 16

$$\Delta_{47\ \text{I-CDES; CDES 90}} = 0.2017 - 36.2 \times (1/T) + 16822 \times (1/T)^2 + 18878240 \times (1/T)^3 - 3064202063 \times (1/T)^4$$

Equation 17

$$\Delta_{48\ \text{CDES 90}} = 0.1642 - 64.1 \times (1/T) + 32920 \times (1/T)^2 - 3140075 \times (1/T)^3 + 354396957 \times (1/T)^4$$

where T is in Kelvin. We also report the inverse of the relationships for ease of use for samples with unknown precipitation temperature in equations 18 and 19.

Equation 18

$$1/T = -0.003728 + 0.04027 \times \Delta_{47\ I-CDES;\ CDES\ 90} - 0.1048 \times (\Delta_{47\ I-CDES;\ CDES\ 90})^2 + 0.134 \times (\Delta_{47\ I-CDES;\ CDES\ 90})^3 - 0.06386 \times (\Delta_{47\ I-CDES;\ CDES\ 90})^4$$

Equation 19

$$1/T = -0.02296 + 0.425 \times \Delta_{48\,CDES\,90} - 2.718 \times (\Delta_{48\,CDES\,90})^2 + 7.936 \times (\Delta_{48\,CDES\,90})^3 - 8.704 \times (\Delta_{48\,CDES\,90})^4$$

To check the robustness of these equations, we solved the Δ_{47}-T equation (equation 16) for 10 °C, yielding a Δ_{47} value of 0.639 ‰. Then, solved the experimentally determined combined Δ_{47}-Δ_{48} regression for Δ_{48} (equation 15) using 0.639 ‰ as the input Δ_{47}. This returned a Δ_{48} value of 0.269 ‰, which is offset by 0.004 ‰ from the Δ_{48} value obtained when solving the Δ_{48}-T equation (equation 17) for 10 °C. While it may seem obvious that these equations would have good agreement, this may not necessarily have been the case given the large amount of data determined here for samples and standards that contributed to the experimental Δ_{47}-Δ_{48} regression not having a constrained relationship to temperature, and it was therefore not used in the Δ_{47}-T and Δ_{48}-T regressions. Additionally, the theoretically based Δ_{47} and Δ_{48} values from Bajnai et al.[8] and this study were not included in the experimentally based Δ_{47}-Δ_{48} regression. Thus, the excellent agreement between the combined experimental Δ_{47}-Δ_{48} regression, and combined Δ_{47}-T and Δ_{48}-T regressions provides evidence that equations 15-19 are robust representations of clumped isotope Δ_{47}-Δ_{48}, Δ_{47}-T, and Δ_{48}-T quasi-equilibrium relationships.

4.6 Comparison of Devils Hole Δ_{47} and Δ_{48}

There are multiple lines of evidence that Devils Hole calcite has achieved very close to oxygen and clumped isotope equilibrium values[35,44] and has a well-constrained precipitation temperature of 33.7 °C[49–52]; therefore, samples from Devils Hole have been used to anchor clumped isotope equilibrium regressions[5,8,10], including in this study. To further constrain Δ_{47} and Δ_{48} values for Devils Hole, replicate-level values from this study were compared to previously published replicate-level values from Bajnai et al.[44] and Fiebig et al.[10]. This study used four samples from core DH-2, spanning 146-176 ka.[34] Bajnai et al.[44] used ten samples from cores DH-11, DHC2-8, and DHC2-3, spanning 4.5-508 ka. Fiebig et al.[10] used four samples from core DHC2-8, all of which were dated to 4.5-16.9 ka. The replicate pools from these three studies were compared using an ANOVA (Table S8), which is a statistical test comparing whether population means are significantly different. The mean Δ_{48} values from all three studies were statistically indistinguishable ($P = 0.71$; $F = 0.34$; Table S8). In contrast, the mean Δ_{47} values from this study and Bajnai et al.[44] were significantly different ($p < 0.0001$), as were mean Δ_{47} values from this study and Fiebig et al.[10] ($p < 0.0001$). The Devils Hole mean Δ_{47} value offset between this study and Bajnai et al.[44] is 0.012 ‰, and 0.018 ‰ between this study and Fiebig et al.[10] (Table 6). For comparison, the largest offset in replicated standard values between this study, Fiebig et al.[7], and Bajnai et al.[8]

was 0.012 ‰ (Table 3), thus, the observed offset in Devils Hole Δ_{47} values could be from analytical error.

It is unlikely that the offsets are the result of Devils Hole samples exhibiting kinetic effects from CO_2 degassing from groundwater, which is observed in other speleothems[19,20,24,53–55]. Clumped isotope values that exhibit kinetic effects from degassing result in decreased Δ_{47} values and increased Δ_{48} values, with an approximately linear early departure from equilibrium that has a slope of ~-0.793[8,24]. The samples from Devils Hole do not follow this trend, as was concluded in Bajnai et al.[44] and here (red arrow in Figure 8). Although we cannot preclude the possibility there are small, yet resolvable differences in Devils Hole clumped isotope values from samples of different ages given that we did not measure the same samples, the evidence here does not provide sufficient evidence to support that conclusion.

The combined average Δ_{47} value from all replicates from samples in this study, Bajnai et al.[44], and Fiebig et al.[10], yielded a Δ_{47} value of 0.571 ± 0.001 ‰, which yields a temperature value of 33.9 ± 0.3 ºC from equation 18. The combined average Δ_{48} value 0.238 ± 0.007 yields a temperature value of 30.8 ± 6.8 ºC when input into equation 19. Both Δ_{47} and Δ_{48} reconstructed temperatures values are congruent with measured temperature values from Devils Hole ranging from 32.8-34.3 ºC[49–52]. This provides further evidence that the observed interlaboratory offsets in Devils Hole samples are likely caused analytical error and/or error from data normalization, and the average interlaboratory Δ_{47} and Δ_{48} values for Devils Hole (Table 6) provide accurate equilibrium clumped isotope values for 33.7 ºC.

5. CONCLUSIONS

This study, which contains 5,465 Δ_{47} and 3,400 Δ_{48} measurements of standards and samples, helps to establish Δ_{48} values that can be used in carbonate standard-based standardization. Our data supports previous Δ_{47} research[26,27,32,43] that carbonate-based standardization is a robust technique, and demonstrate that carbonate standard-based standardization produces statistically indistinguishable Δ_{48} data on varying instrumentation. Interlaboratory reproducibility of Δ_{48} values would likely be improved by the universal application of carbonate-based standardization using agreed upon carbonate standard values.

We have further constrained the equilibrium Δ_{47}-Δ_{48} relationship with experimental values for standards and samples and formed a combined experimental regression with data from this study and previously published work. We constructed equilibrium Δ_{47}-T and Δ_{48}-T regressions using experimental and theoretically-based values and formed combined regressions using this study and previously published work. We compared Δ_{47}-Δ_{48} values for Devils Hole calcite from this study and previously

published work and determined that the overall combined average Δ_{47}- and Δ_{48}-reconstructed temperatures align with measured values of 33.7 ^{o}C.

Data Accessibility Statement

All code and raw data used in analyses are available for review at https://github.com/Tripati-Lab/Lucarelli-et-al. Upon acceptance for publication, code and raw data will be permanently archived at Dryad, a static link provided in the manuscript, and this section updated.

Acknowledgements

We thank laboratory members past and present for their work running standards, efforts in data entry, and contributions to discussions. This work was funded by DOE BES grant DE-FG02-13ER16402. HMC was supported through a postdoctoral fellowship by the Institutional Research and Academic Career Development Awards (IRACDA) program at UCLA (Award # K12 GM106996).

References

1. Ghosh, P. *et al.* 13C–18O bonds in carbonate minerals: A new kind of paleothermometer. *Geochimica et Cosmochimica Acta* **70**, 1439–1456 (2006).
2. Schauble, E. A., Ghosh, P. & Eiler, J. M. Preferential formation of 13C–18O bonds in carbonate minerals, estimated using first-principles lattice dynamics. *Geochimica et Cosmochimica Acta* **70**, 2510–2529 (2006).
3. Guo, W., Mosenfelder, J. L., Goddard, W. A. & Eiler, J. M. Isotopic fractionations associated with phosphoric acid digestion of carbonate minerals: Insights from first-principles theoretical modeling and clumped isotope measurements. *Geochimica et Cosmochimica Acta* **73**, 7203–7225 (2009).
4. Hill, P. S., Tripati, A. K. & Schauble, E. A. Theoretical constraints on the effects of pH, salinity, and temperature on clumped isotope signatures of dissolved inorganic carbon species and precipitating carbonate minerals. *Geochimica et Cosmochimica Acta* **125**, 610–652 (2014).
5. Tripati, A. K. *et al.* Beyond temperature: Clumped isotope signatures in dissolved inorganic carbon species and the influence of solution chemistry on carbonate mineral composition. *Geochimica et Cosmochimica Acta* **166**, 344–371 (2015).
6. Guo, Y., Deng, W. & Wei, G. Kinetic effects during the experimental transition of aragonite to calcite in aqueous solution: Insights from clumped and oxygen isotope signatures. *Geochimica et Cosmochimica Acta* **248**, 210–230 (2019).

7. Fiebig, J. *et al.* Combined high-precision ∆48 and ∆47 analysis of carbonates. *Chemical Geology* **522**, 186–191 (2019).
8. Bajnai, D. *et al.* Dual clumped isotope thermometry resolves kinetic biases in carbonate formation temperatures. *Nat Commun* **11**, 4005 (2020).
9. Swart, P. K. *et al.* A calibration equation between Δ_{48} values of carbonate and temperature. *Rapid Commun Mass Spectrom* **35**, (2021).
10. Fiebig, J. *et al.* Calibration of the dual clumped isotope thermometer for carbonates. *Geochimica et Cosmochimica Acta* S0016703721004208 (2021) doi:10.1016/j.gca.2021.07.012.
11. Eiler, J. M. & Schauble, E. 18O13C16O in Earth's atmosphere. *Geochimica et Cosmochimica Acta* **68**, 4767–4777 (2004).
12. Eiler, J. M. "Clumped-isotope" geochemistry—The study of naturally-occurring, multiply-substituted isotopologues. *Earth and Planetary Science Letters* **262**, 309–327 (2007).
13. Urey, H. C. The thermodynamic properties of isotopic substances. *J. Chem. Soc.* 562 (1947) doi:10.1039/jr9470000562.
14. Passey, B. H. & Henkes, G. A. Carbonate clumped isotope bond reordering and geospeedometry. *Earth and Planetary Science Letters* **351–352**, 223–236 (2012).
15. Henkes, G. A. *et al.* Temperature evolution and the oxygen isotope composition of Phanerozoic oceans from carbonate clumped isotope thermometry. *Earth and Planetary Science Letters* **490**, 40–50 (2018).
16. Huntington, K. W., Wernicke, B. P. & Eiler, J. M. Influence of climate change and uplift on Colorado Plateau paleotemperatures from carbonate clumped isotope thermometry. *Tectonics* **29**, 2009TC002449 (2010).
17. Lechler, A. R., Niemi, N. A., Hren, M. T. & Lohmann, K. C. Paleoelevation estimates for the northern and central proto-Basin and Range from carbonate clumped isotope thermometry: Δ_{47} PALEOALTIMETRY OF BASIN AND RANGE. *Tectonics* **32**, 295–316 (2013).
18. Eagle, R. A. *et al.* Body temperatures of modern and extinct vertebrates from 13C-18O bond abundances in bioapatite. *Proceedings of the National Academy of Sciences* **107**, 10377–10382 (2010).
19. Affek, H. P., Bar-Matthews, M., Ayalon, A., Matthews, A. & Eiler, J. M. Glacial/interglacial temperature variations in Soreq cave speleothems as recorded by 'clumped isotope' thermometry. *Geochimica et Cosmochimica Acta* **72**, 5351–5360 (2008).
20. Daëron, M. *et al.* 13C18O clumping in speleothems: Observations from natural caves and precipitation experiments. *Geochimica et Cosmochimica Acta* **75**, 3303–3317 (2011).

21. Thiagarajan, N., Adkins, J. & Eiler, J. Carbonate clumped isotope thermometry of deep-sea corals and implications for vital effects. *Geochimica et Cosmochimica Acta* **75**, 4416–4425 (2011).
22. Kimball, J., Eagle, R. & Dunbar, R. Carbonate “clumped” isotope signatures in aragonitic scleractinian and calcitic gorgonian deep-sea corals. *Biogeosciences* **13**, 6487–6505 (2016).
23. Saenger, C. *et al.* Carbonate clumped isotope variability in shallow water corals: Temperature dependence and growth-related vital effects. *Geochimica et Cosmochimica Acta* **99**, 224–242 (2012).
24. Guo, W. Kinetic clumped isotope fractionation in the DIC-H2O-CO2 system: Patterns, controls, and implications. *Geochimica et Cosmochimica Acta* **268**, 230–257 (2020).
25. Hill, P. S., Schauble, E. A. & Tripati, A. Theoretical constraints on the effects of added cations on clumped, oxygen, and carbon isotope signatures of dissolved inorganic carbon species and minerals. *Geochimica et Cosmochimica Acta* **269**, 496–539 (2020).
26. Dennis, K. J., Affek, H. P., Passey, B. H., Schrag, D. P. & Eiler, J. M. Defining an absolute reference frame for ‘clumped’ isotope studies of CO2. *Geochimica et Cosmochimica Acta* **75**, 7117–7131 (2011).
27. Bernasconi, S. M. *et al.* InterCarb: A Community Effort to Improve Interlaboratory Standardization of the Carbonate Clumped Isotope Thermometer Using Carbonate Standards. *Geochem Geophys Geosyst* **22**, (2021).
28. Zaarur, S., Affek, H. P. & Brandon, M. T. A revised calibration of the clumped isotope thermometer. *Earth and Planetary Science Letters* **382**, 47–57 (2013).
29. Burgener, L. *et al.* Variations in soil carbonate formation and seasonal bias over >4 km of relief in the western Andes (30°S) revealed by clumped isotope thermometry. *Earth and Planetary Science Letters* **441**, 188–199 (2016).
30. Peral, M. *et al.* Updated calibration of the clumped isotope thermometer in planktonic and benthic foraminifera. *Geochimica et Cosmochimica Acta* **239**, 1–16 (2018).
31. Meckler, A. N., Ziegler, M., Millán, M. I., Breitenbach, S. F. M. & Bernasconi, S. M. Long-term performance of the Kiel carbonate device with a new correction scheme for clumped isotope measurements: Performance and correction of Kiel clumped isotope measurements. *Rapid Commun. Mass Spectrom.* **28**, 1705–1715 (2014).
32. Upadhyay, D. *et al.* Carbonate clumped isotope analysis (Δ_{47}) of 21 carbonate standards determined via gas-source isotope-ratio mass spectrometry on four instrumental configurations using carbonate-based standardization and multiyear data sets. *Rapid Commun Mass Spectrom* **35**, (2021).

33. Tripati, A. K. *et al.* 13C–18O isotope signatures and ‘clumped isotope’ thermometry in foraminifera and coccoliths. *Geochimica et Cosmochimica Acta* **74**, 5697–5717 (2010).
34. Winograd, I. J. *et al.* Continuous 500,000-Year Climate Record from Vein Calcite in Devils Hole, Nevada. *Science* **258**, 255–260 (1992).
35. Coplen, T. B. Calibration of the calcite–water oxygen-isotope geothermometer at Devils Hole, Nevada, a natural laboratory. *Geochimica et Cosmochimica Acta* **71**, 3948–3957 (2007).
36. Kluge, T., Affek, H. P., Dublyansky, Y. & Spötl, C. Devils Hole paleotemperatures and implications for oxygen isotope equilibrium fractionation. *Earth and Planetary Science Letters* **400**, 251–260 (2014).
37. Winograd, I. J., Coplen, T. B., Szabo, B. J. & Riggs, A. C. A 250,000-Year Climatic Record from Great Basin Vein Calcite: Implications for Milankovitch Theory. *Science* **242**, 1275–1280 (1988).
38. Passey, B. H., Levin, N. E., Cerling, T. E., Brown, F. H. & Eiler, J. M. High-temperature environments of human evolution in East Africa based on bond ordering in paleosol carbonates. *Proceedings of the National Academy of Sciences* **107**, 11245–11249 (2010).
39. John, C. M. & Bowen, D. Community software for challenging isotope analysis: First applications of ‘Easotope’ to clumped isotopes: Community software for challenging isotope analysis. *Rapid Commun. Mass Spectrom.* **30**, 2285–2300 (2016).
40. Brand, W. A., Assonov, S. S. & Coplen, T. B. Correction for the 17O interference in δ(13C) measurements when analyzing CO2 with stable isotope mass spectrometry (IUPAC Technical Report). *Pure and Applied Chemistry* **82**, 1719–1733 (2010).
41. Daëron, M., Blamart, D., Peral, M. & Affek, H. P. Absolute isotopic abundance ratios and the accuracy of Δ47 measurements. *Chemical Geology* **442**, 83–96 (2016).
42. Wang, Z., Schauble, E. A. & Eiler, J. M. Equilibrium thermodynamics of multiply substituted isotopologues of molecular gases. *Geochimica et Cosmochimica Acta* **68**, 4779–4797 (2004).
43. Bernasconi, S. M. *et al.* Reducing Uncertainties in Carbonate Clumped Isotope Analysis Through Consistent Carbonate-Based Standardization. *Geochem. Geophys. Geosyst.* **19**, 2895–2914 (2018).
44. Bajnai, D. *et al.* Devils Hole Calcite Was Precipitated at ±1°C Stable Aquifer Temperatures During the Last Half Million Years. *Geophys Res Lett* **48**, (2021).
45. Daëron, M. Full Propagation of Analytical Uncertainties in Δ_{47} Measurements. *Geochem Geophys Geosyst* **22**, (2021).
46. Kocken, I. J., Müller, I. A. & Ziegler, M. Optimizing the Use of Carbonate Standards to Minimize Uncertainties in Clumped Isotope Data. *Geochem. Geophys. Geosyst.* **20**, 5565–5577 (2019).

47. Müller, I. A. *et al.* Clumped isotope fractionation during phosphoric acid digestion of carbonates at 70 °C. *Chemical Geology* **449**, 1–14 (2017).
48. Daëron, M. *et al.* Most Earth-surface calcites precipitate out of isotopic equilibrium. *Nat Commun* **10**, 429 (2019).
49. Miller, R. Miller, Robert Rush. "The cyprinodont fishes of the Death Valley system of eastern California and southwestern Nevada. *Miscellaneous Publications Museum of Zoology, University of Michigan* **68**, (1948).
50. Dudley, W. & Larson, J. D. *Effect of irrigation pumping on desert pupfish habitats in the Ash Meadows, Nye County, Nevada*. (1976).
51. Hoffman, R. *Chronology of diving activities and underground surveys in Devils Hole and Devils Hole Cave, Nye County, Nevada, 1950-86*. (1988).
52. Plummer, L. N., Busenberg, E. & Riggs, A. C. In-situ Growth of Calcite at Devils Hole, Nevada: Comparison of Field and Laboratory Rates to a 500,000 Year Record of Near-Equilibrium Calcite Growth. *Aquatic Geochemistry* **6**, 257–274 (2000).
53. Kluge, T. & Affek, H. P. Quantifying kinetic fractionation in Bunker Cave speleothems using Δ47. *Quaternary Science Reviews* **49**, 82–94 (2012).
54. Affek, H. P. & Zaarur, S. Kinetic isotope effect in CO2 degassing: Insight from clumped and oxygen isotopes in laboratory precipitation experiments. *Geochimica et Cosmochimica Acta* **143**, 319–330 (2014).
55. Guo, W. & Zhou, C. Patterns and controls of disequilibrium isotope effects in speleothems: Insights from an isotope-enabled diffusion-reaction model and implications for quantitative thermometry. *Geochimica et Cosmochimica Acta* **267**, 196–226 (2019).

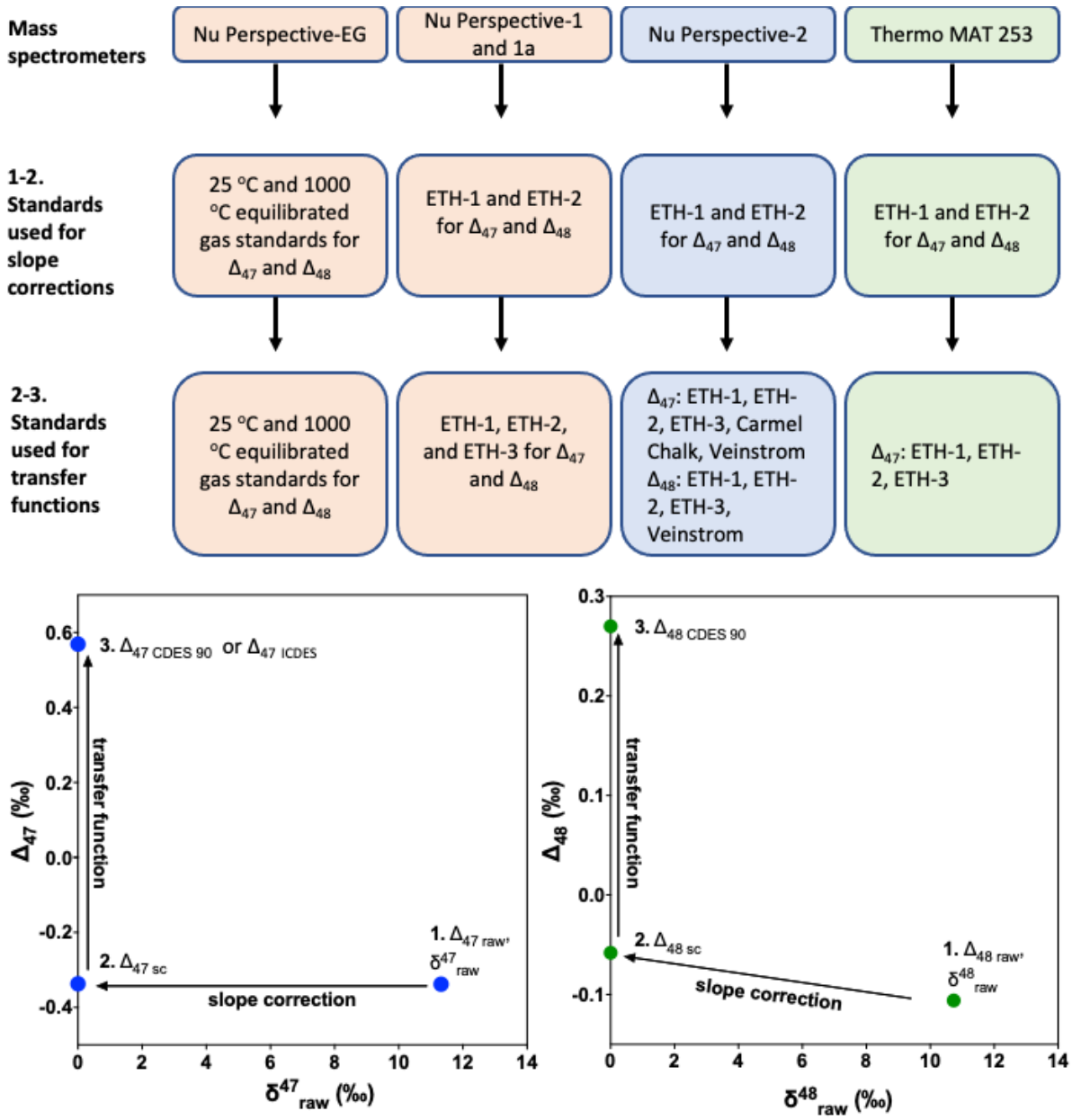

Figure 1. Flow chart indicating which standards are used for data normalization in each instrumental configuration, and how the data is transformed at each step. The bottom two panels are adapted from Dennis et al.[26].

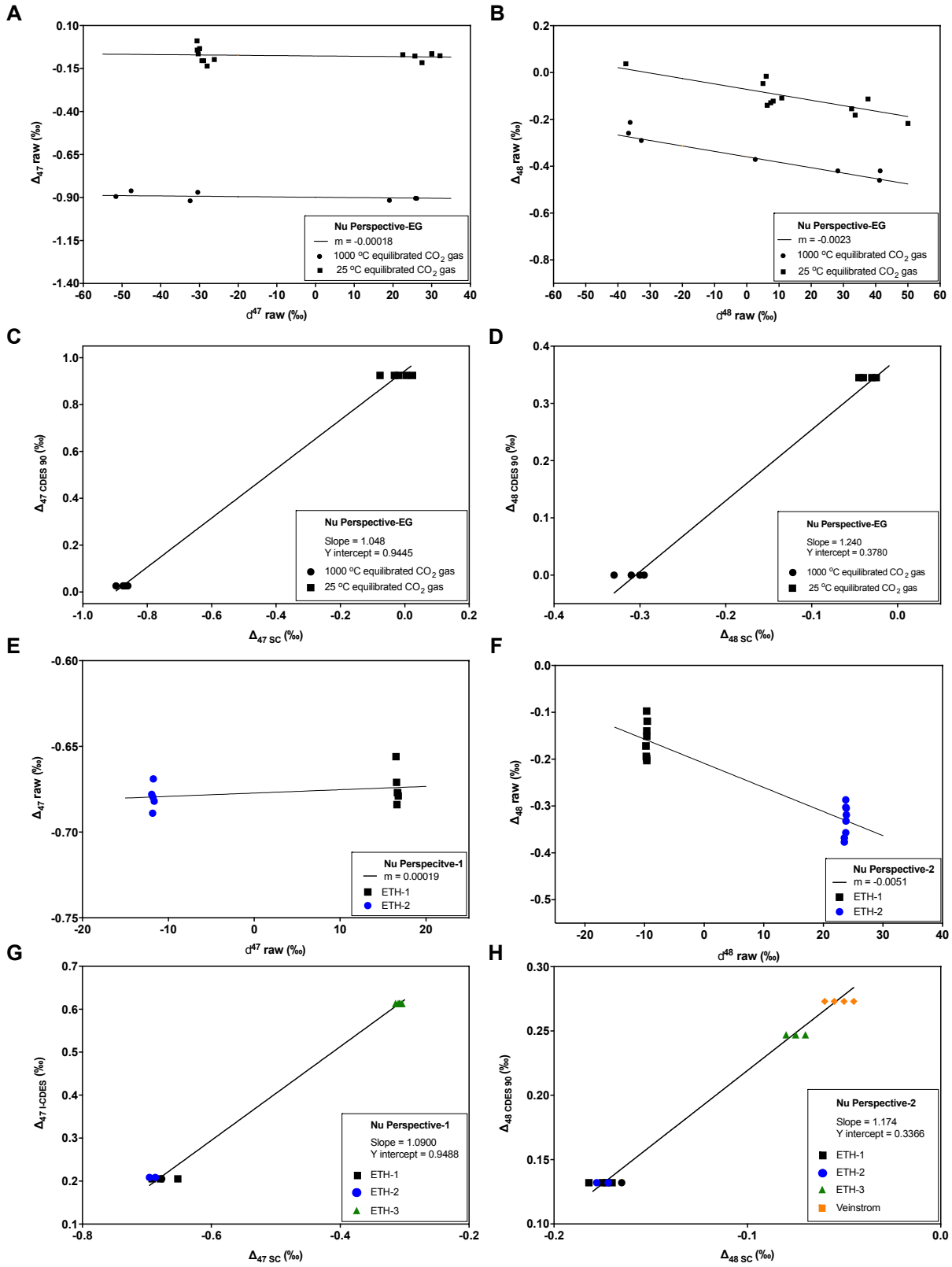

Figure 2. Representative examples of slope corrections and transfer functions performed for data normalization. Panels A) and B) are the slope correction using

equilibrated gas standards on Nu Perspective-EG for δ^{47} versus $\Delta_{47\ raw}$ and δ^{48} and $\Delta_{48\ raw}$, respectively. Panels C) and D) are transfer functions using equilibrated gas standards on Nu Perspective-EG for Δ_{47} and Δ_{48}, respectively. Panels (E) and (F) are the slope correction using carbonate standards ETH-1 and ETH-2 on Nu Perspective-1 for δ^{47} versus $\Delta_{47\ raw}$ and δ^{48} and $\Delta_{48\ raw}$, respectively. Panels (G) and (H) are transfer functions using carbonate standards ETH-1, ETH-2, and ETH-3, and Veinstrom (for Δ_{48} only) on Nu Perspective-1 for Δ_{47} and Δ_{48}, respectively. The slopes are determined on a 10-day moving interval to account for instrument drift and applied to standards and samples. Data normalization is performed similarly on all instruments.

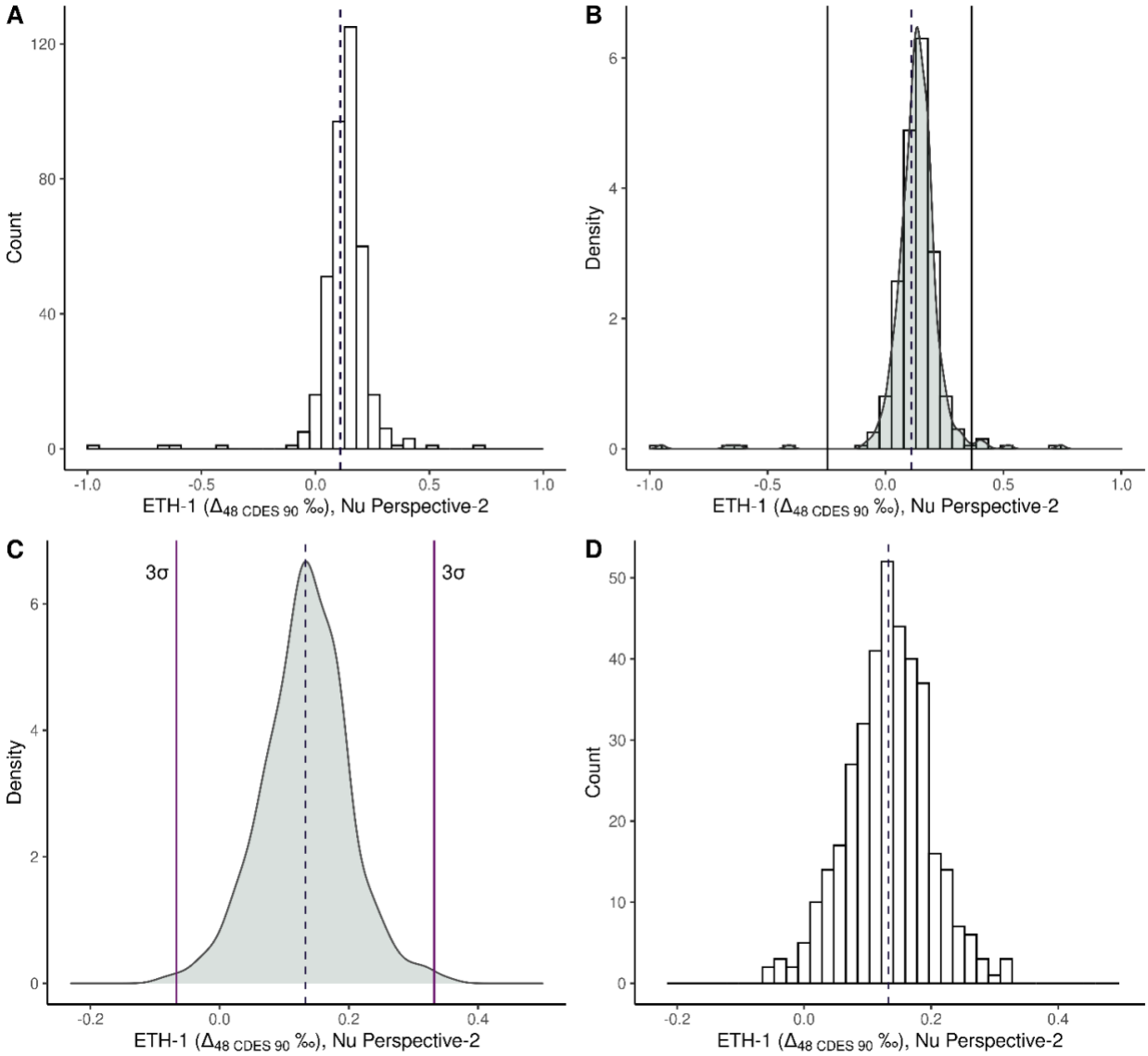

Figure 3. Example of data throughout the quality control process. In all panels, the dashed vertical line represents the mean value of sample replicates. A) Histogram of the raw replicate pool (N = 389, where N is the number of sample replicates). B) Density plot with histogram of the raw replicate pool and first outlier removal for large outliers (solid vertical lines). C) Density plot of the replicate pool following initial exclusions (N = 378); potential cutoff at 3σ (solid vertical lines) is shown. D) Histogram of the final replicate pool following a 3σ exclusion (mean = 0.133 ‰, SD = 0.065, N = 376). Note that the x and y axis scales differ between plots.

A

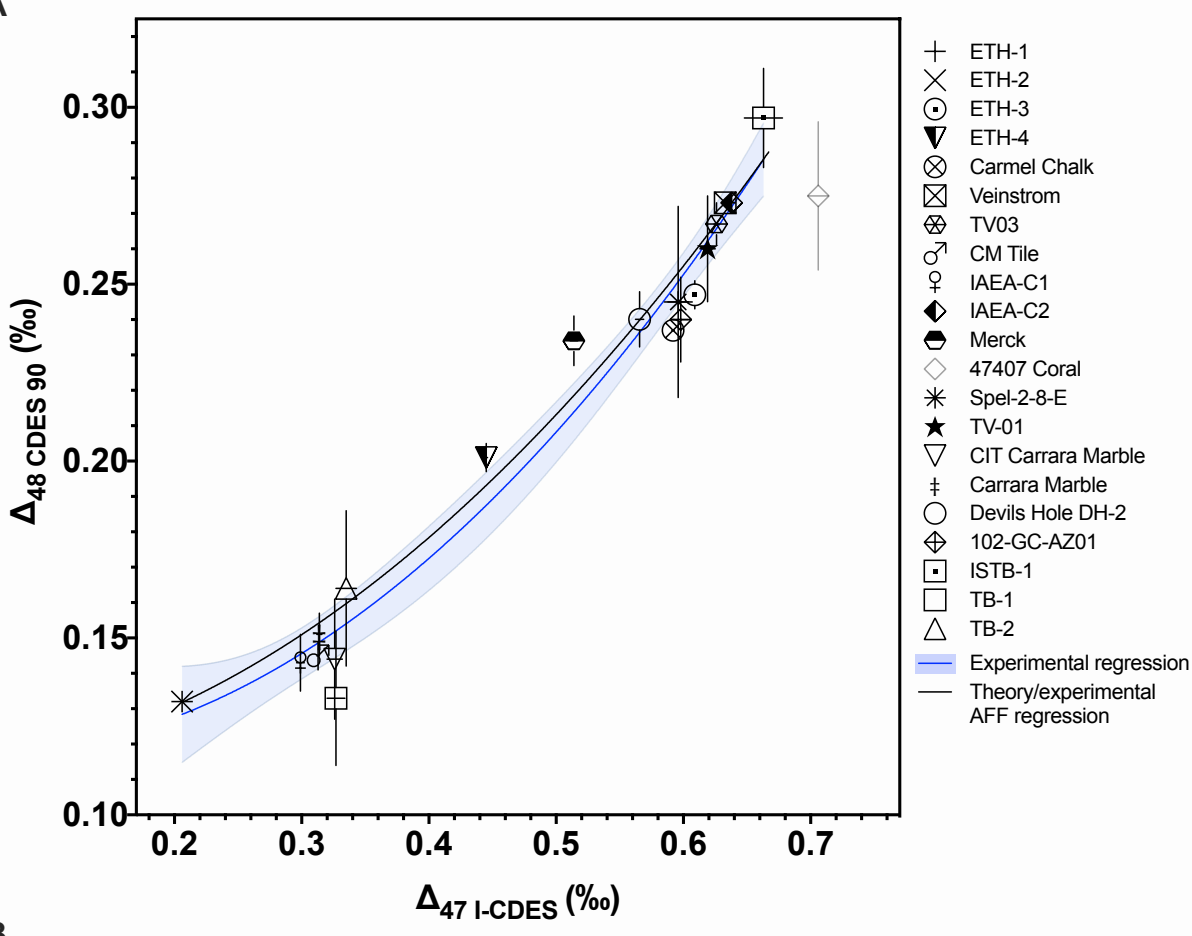
0.30
0.25
0.20
0.15
0.10
0.2
0.3
0.4
0.5
0.6
0.7
Δ48 CDES 90 (‰)
Δ47 I-CDES (‰)
ETH-1
ETH-2
ETH-3
ETH-4
Carmel Chalk
Veinstrom
TV03
CM Tile
IAEA-C1
IAEA-C2
Merck
47407 Coral
Spel-2-8-E
TV-01
CIT Carrara Marble
Carrara Marble
Devils Hole DH-2
102-GC-AZ01
ISTB-1
TB-1
TB-2
Experimental regression
Theory/experimental AFF regression

B

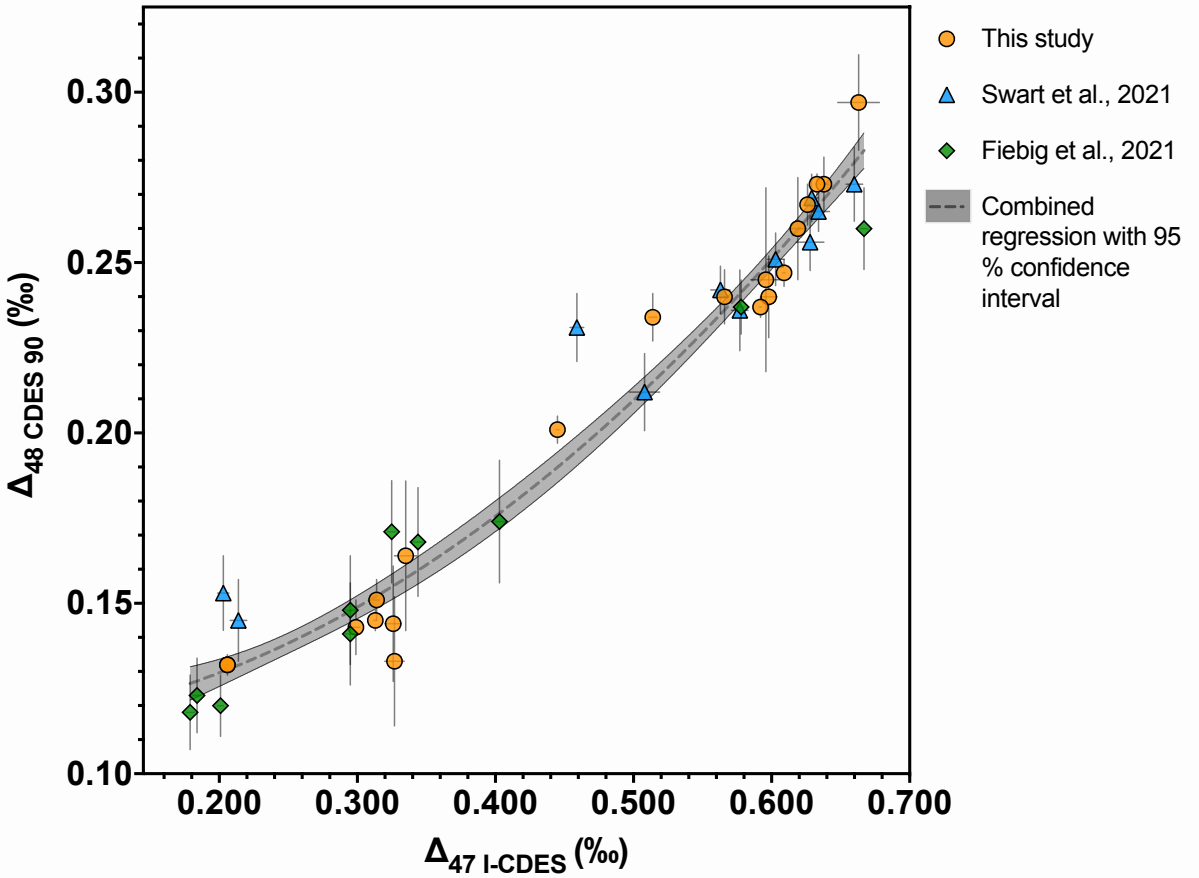
0.30
0.25
0.20
0.15
0.10
0.200
0.300
0.400
0.500
0.600
0.700
Δ48 CDES 90 (‰)
Δ47 I-CDES (‰)
This study
Swart et al., 2021
Fiebig et al., 2021
Combined regression with 95 % confidence interval

Figure 4. A) Plot showing for Δ_{47}-Δ_{48} values for 21 samples including standards and Devils Hole (DH-2) cave calcite. A second order polynomial was fitted through all samples, with the exception of 47407 Coral, which may express kinetic bias. The light blue shading indicates the 95 % confidence interval. Also shown is an equilibrium regression calculated using theoretical calcite equilibrium Δ_{63} and Δ_{64}[4,5] combined with experimental AFFs to determine Δ_{47}-Δ_{48} values. Error bars indicate 1 SE. B) Experimental Δ_{47}-Δ_{48} data from this study, Swart et al.[9], and Fiebig et al.[10] The data from this study are the same as for panel A, with the exception of 47407 Coral. The individual regressions fit through each dataset were determined to be statistically indistinguishable (P = 0.86; F = 0.43; Table S7), and a combined data regression was determined including all three datasets. The grey shading indicates the 95 % confidence interval for the combined regression.

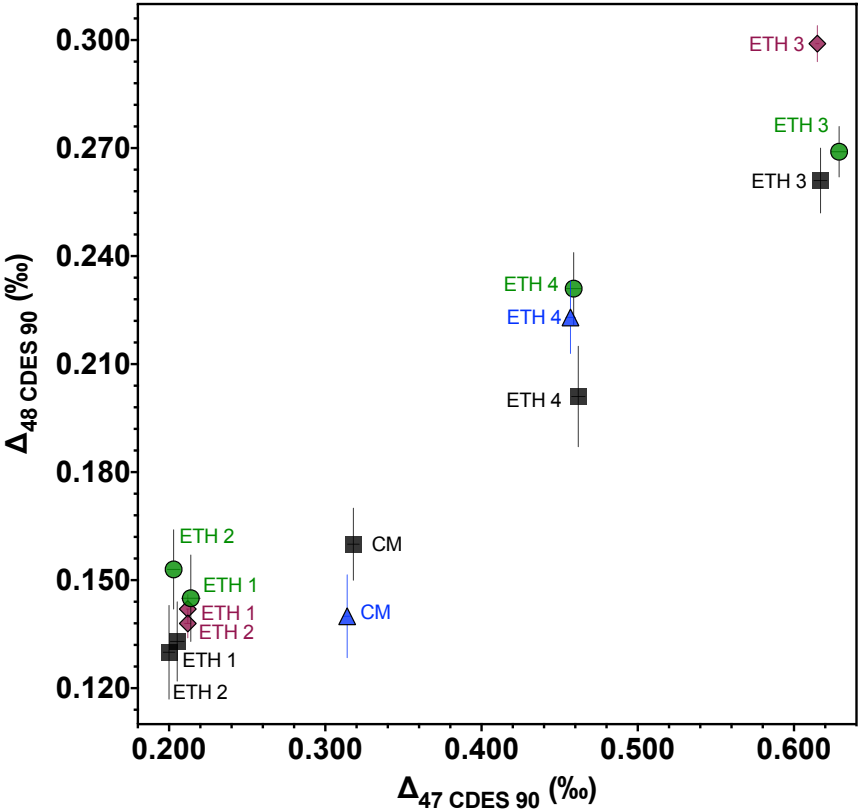

This study; Nu Perspective-EG

Fiebig et al., 2019

Fiebig et al., 2019; Bajnai et al., 2020

Swart et al., 2021

Figure 5. Plot showing comparison between Δ_{47}-Δ_{48} values for ETH-1, ETH-2, ETH-3, ETH-4, and Carrara Marble (CM) from Nu Perspective-EG from this study with values from Fiebig et al.[7], Bajnai et al.[8], and Swart et al.[9] All data in this plot were standardized with 25 ^{o}C and 1000 ^{o}C equilibrated gas-based standardization. Error bars indicate 1 SE.

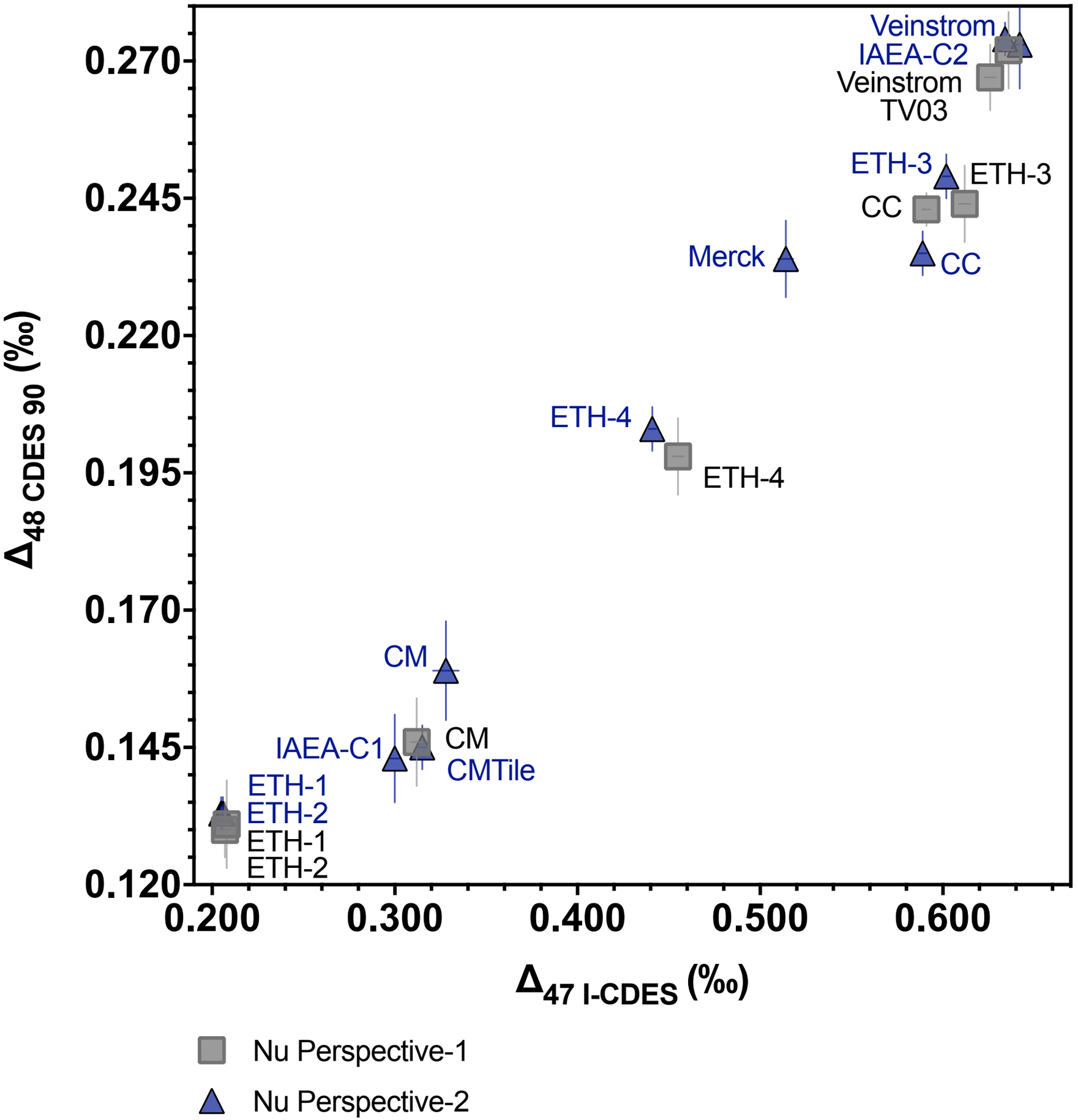
Veinstrom
IAEA-C2
Veinstrom
TV03
ETH-3
ETH-3
CC
CC
Merck
ETH-4
ETH-4
CM
CM
CMTile
IAEA-C1
ETH-1
ETH-2
ETH-1
ETH-2
0.270
0.245
0.220
0.195
0.170
0.145
0.120
0.200
0.300
0.400
0.500
0.600
Δ48 CDES 90 (‰)
Δ47 I-CDES (‰)
Nu Perspective-1
Nu Perspective-2

Figure 6. Δ_{47}-Δ_{48} values for standards and samples determined using carbonate-based standardization on Nu Perpective-1 and Nu Perspective-2. Error bars indicate 1 SE.

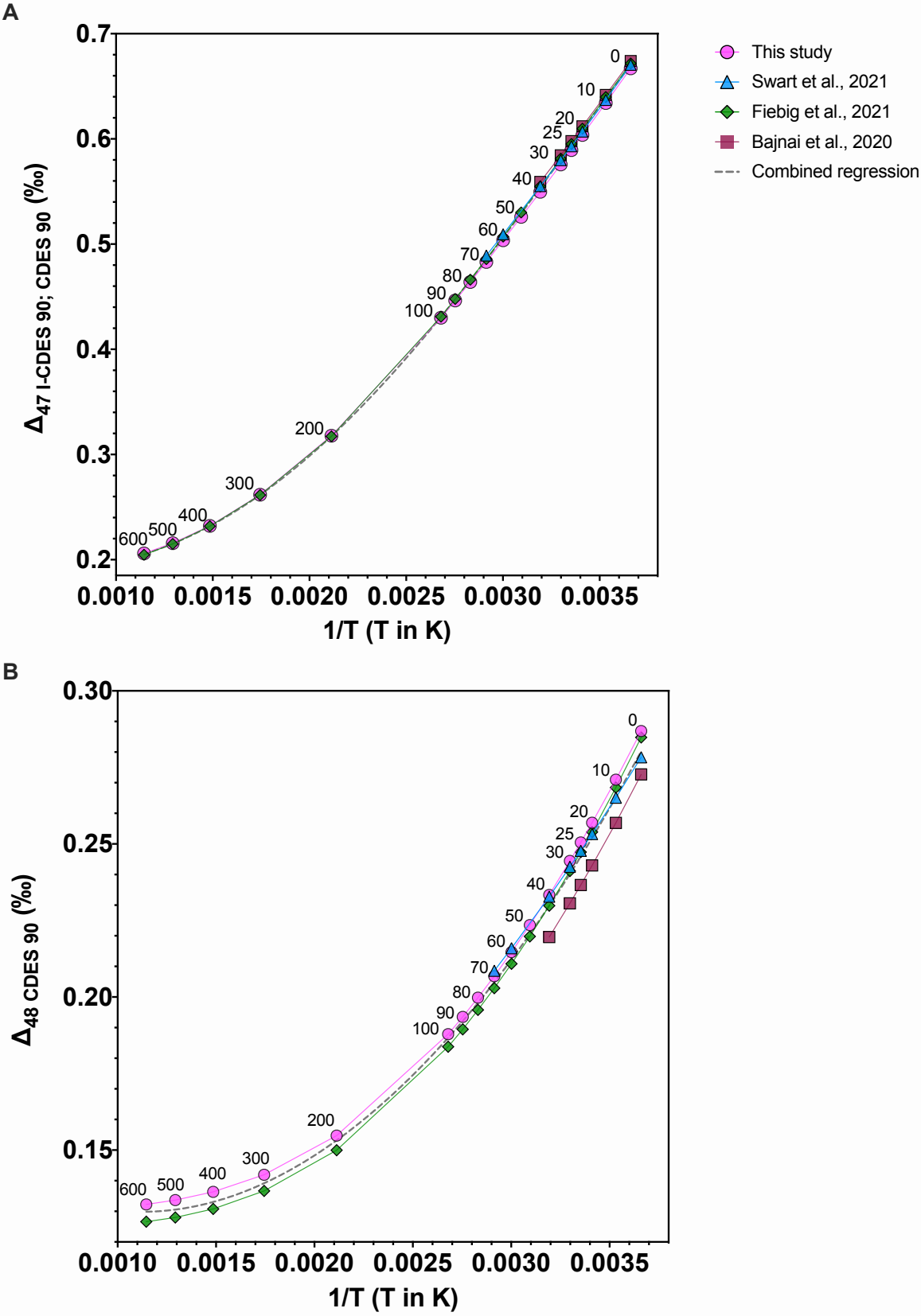
A
0.7
0.6
0.5
0.4
0.3
0.2
Δ_{47} I-CDES 90; CDES 90 (‰)
0.0010
0.0015
0.0020
0.0025
0.0030
0.0035
1/T (T in K)
0
10
20
25
30
40
50
60
70
80
90
100
200
300
400
500
600
This study
Swart et al., 2021
Fiebig et al., 2021
Bajnai et al., 2020
Combined regression
B
0.30
0.25
0.20
0.15
Δ_{48} CDES 90 (‰)
0.0010
0.0015
0.0020
0.0025
0.0030
0.0035
1/T (T in K)
0
10
20
25
30
40
50
60
70
80
90
100
200
300
400
500
600

Figure 7. A) Δ_{47}-T and B) Δ_{48}-T regressions from this study and Bajnai et al.[8] that rely on calcite Δ_{63}-Δ_{64} equilibrium theory and experimental AFFs, and regressions from Swart et al.[9] and Fiebig et al.[10] that rely on experimentally constrained values. A combined regression for all datasets is represented by the gray dashed line. Numbers by the data points indicate temperature in Celsius.

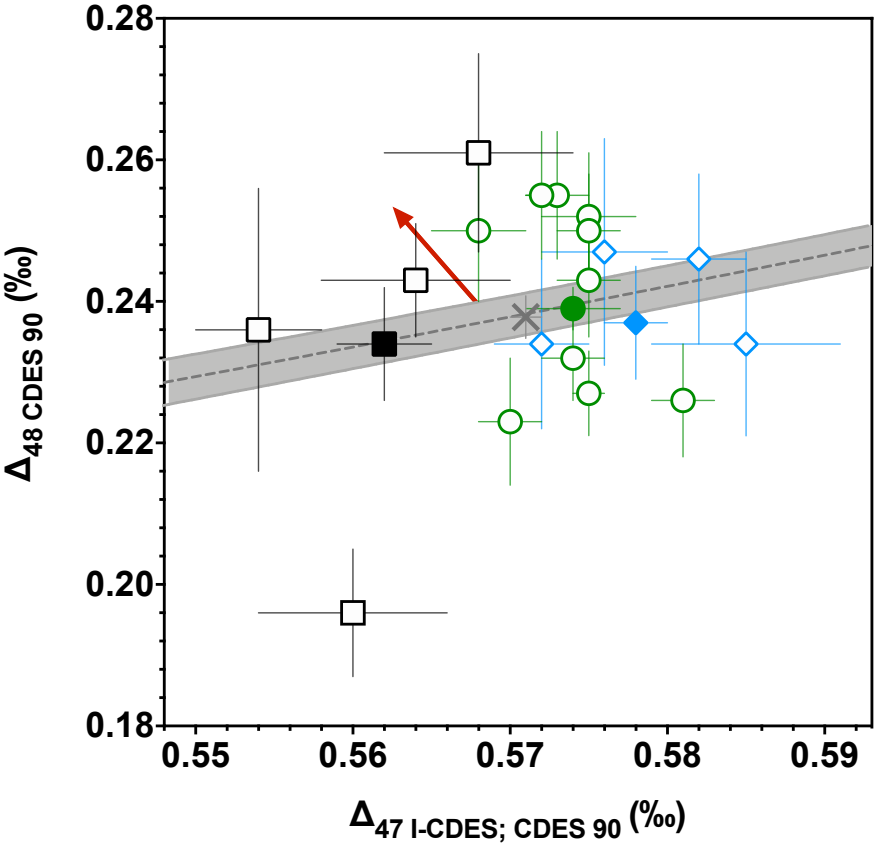

This study

Bajnai et al., 2021

Fiebig et al., 2021

Solid points are average values

Interlaboratory combined average

Figure 8. Plot showing Δ_{47}-Δ_{48} values for Devils Hole cave calcite determined in this study, Bajnai et al.[44] and Fiebig et al.[10] The open points indicate individual samples, and solid points are the overall average from each study. The gray X is the combined average from all datasets. The gray dashed line is the combined experimental regression (equation 15 with the 95 % confidence interval).

Table 1. Description of the mineralogy and origin for samples and standards analyzed in this study (Upadhyay et al., 2021; Chang et al., 2020; Bernasconi et al., 2018), including 4 samples of Devils Hole calcite. Uranium-series ages for Devils Hole vein calcite were determined by Winograd et al. (2006).

Standard	Mineralogy	Origin
102-GC-AZ01	calcite	Vein carbonate from Grand Canyon
Carmel Chalk	calcite	Chalk
Carrara Marble	calcite	Collected in Carrara, Tuscany, Italy.
CM Tile	calcite	Homogenized version of Carrara Marble (UCLA)
47407 Coral	aragonite	Deep sea coral, *Desmophyllum*
DH-2-10	calcite	Devils Hole - U.S. Geological Survey, Ash Meadows, Nevada. Core DH-2. 172 ± 4 ka
DH-2-11	calcite	Devils Hole - U.S. Geological Survey, Ash Meadows, Nevada. Core DH-2. 163 ± 5 ka
DH-2-12	calcite	Devils Hole - U.S. Geological Survey, Ash Meadows, Nevada. Core DH-2. 157 ± 5 ka
DH-2-13	calcite	Devils Hole - U.S. Geological Survey, Ash Meadows, Nevada. Core DH-2. 151 ± 4 ka
ETH-1	calcite	Carrara Marble, heated to 600°C at 155 MPa for 10 hours, sent from ETH Zurich
ETH-2	calcite	Reagent grade synthetic, subjected to same treatment as ETH-1, sent from ETH Zurich
ETH-3	calcite	Upper Cretaceous chalk (mostly coccoliths), Isle of Rügen, Germany, sent from ETH Zurich
ETH-4	calcite	Same reagent grade synthetic as ETH-2, but unheated, sent from ETH Zurich
IAEA-C1	calcite	Carrara Marble, from International Atomic Energy Agency
IAEA-C2	travertine	Collected in Bavaria. From International Atomic Energy Agency
ISTB-1	calcite	Speleothem from Yichang, Hubei province, China
Mallinckrodt	calcite	Synthetic, from Mallinckrodt Baker, Inc.
MERCK	calcite	Synthetic, from International Atomic Energy Agency
NBS 19	calcitic marble	Carrara Marble, from National Bureau of Standards
Spel 2-8-E	calcite	Speleothem
SRM 88B	dolomitic limestone	Collected from mine site near Skokie, Illinois, USA
TB-1	marble	Marble rock of marine origin from Quyang, Hebei province, China
TB-2	calcite	Hydrothermal calcite from Yanji, Jilin province, China
TV01	calcite	Travertine tile
TV03	calcite	Travertine tile
Veinstrom	calcite	Shallow carbonate vein collected from Tempiute Mountain, Nevada

Table 2. Description of mass spectrometer configurations used in this study.

Configuration	Mass spectrometer model	Acid digestion temperature	Acid Digestion System, sample size	m/z 44 ion beam intensity	Integration time	Use of equilibrated gas-based corrections	Use of carbonate-based corrections
Nu Perspective- EG	Nu Instruments Perspective	90 °C	Common acid bath, 0.45-0.60	80 nA before 6/2017, 60 nA after	1600 s	Yes, 25 and 1000 °C gases	No
Nu Perspective-1	Nu Instruments Perspective	90 °C	Common acid bath,0.45-0.60	80 nA before 6/2017, 60 nA after	1600 s	No	Yes
Nu Perspective -1a	Nu Instruments Perspective	90 °C	Common acid bath, 0.45-0.60	80-30 nA	1200 s	No	Yes
Nu Perspective-2	Nu Instruments Perspective	70 °C	Nu Carb, 0.45-0.60	80-30 nA	1200 s	No	Yes
MAT 253	Thermo Finnigan MAT 253	90 °C	Common acid bath, 5-7 mg	16 V	720 s	No	Yes

Table 3. Δ_{47} and Δ_{48} for samples and standards analyzed on Nu Perspective-EG. All data in this table was standardized using only 25 and 1000 °C equilibrated gases. Results are compared to values from Fiebig et al., (2019), Bajnai et al. (2020), and Swart et al. (2021).

	This study, Nu Perspective-EG						Bernasconi et al., 2021			Fiebig et al., 2019					Fiebig et al., 2019; Bajnai et al., 2020					Swart et al., 2021				
Sample	**N**	**Δ_{47} CDES 90 (‰)**	**Δ_{47} SE**	**N**	**Δ_{48} CDES 90 (‰)**	**Δ_{48} SE**	**N**	**Δ_{47} CDES 90 (‰)**	**Δ_{47} SE**	**N**	**Δ_{47} CDES 90 (‰)**	**Δ_{47} SE**	**Δ_{48} CDES 90 (‰)**	**Δ_{48} SE**	**N**	**Δ_{47} CDES 90 (‰)**	**Δ_{47} SE**	**Δ_{48} CDES 90 (‰)**	**Δ_{48} SE**	**N**	**Δ_{47} CDES 90 (‰)**	**Δ_{47} SE**	**Δ_{48} CDES 90 (‰)**	**Δ_{48} SE**
Carrara Mar	62	0.318	0.004	64	0.160	0.010				12	0.314	0.003	0.140	0.012										
ETH-1	36	0.205	0.004	44	0.133	0.011	232	0.205	0.002						78	0.212	0.001	0.142	0.004	19	0.214	0.006	0.145	0.012
ETH-2	30	0.200	0.004	36	0.130	0.013	215	0.208	0.001						71	0.212	0.002	0.138	0.004	14	0.203	0.004	0.153	0.011
ETH-3	35	0.617	0.003	45	0.261	0.009	264	0.613	0.001						74	0.615	0.001	0.299	0.005	20	0.629	0.005	0.269	0.007
ETH-4	36	0.462	0.004	45	0.201	0.014	162	0.450	0.002	11	0.457	0.003	0.223	0.010						14	0.459	0.005	0.231	0.010
TV03	56	0.637	0.005	55	0.269	0.007																		
Veinstrom	69	0.643	0.004	74	0.263	0.010																		

Table 4. Individual instrument and longterm combined average Δ_{47} and Δ_{48} values for all samples and standards analyzed in this study. Δ_{48} values from MAT 253 (gray columns) were not included in the combined instrument average and are given for informational purposes only. Samples with an asterisk (*) were used as standards in corrections for data normalization.

	Nu Perspective 1								**Nu Perspective 2**								**MAT 253**								**Combined average (Nu Perspective 1, Nu Perspective 2, MAT 253**				**Combined average (Nu Perspective 1, Nu Perspective 1a, Nu Perspective 2)**			
Standard	**Δ_{47} I-CDES (‰)**	N	**Δ_{47} SD**	**Δ_{47} SE**	**Δ_{48} CDES 90 (‰)**	N	**Δ_{48} SD**	**Δ_{48} SE**	**Δ_{47} I-CDES (‰)**	N	**Δ_{47} SD**	**Δ_{47} SE**	**Δ_{48} CDES 90 (‰)**	N	**Δ_{48} SD**	**Δ_{48} SE**	**Δ_{47} I-CDES (‰)**	N	**Δ_{47} SD**	**Δ_{47} SE**	**Δ_{48} CDES 90 (‰)**	N	**Δ_{48} SD**	**Δ_{48} SE**	**Δ_{47} I-CDES (‰)**	N	**Δ_{47} SD**	**Δ_{47} SE**	**Δ_{48} CDES 90 (‰)**	N	**Δ_{48} SD**	**Δ_{48} SE**
102-GC-AZ01																									0.598	24	0.028	0.006	0.240	24	0.057	0.012
Carmel Chalk	0.591	94	0.017	0.002	0.243	69	0.028	0.003	*0.589	248	0.026	0.002	0.235	250	0.062	0.004	0.594	282	0.021	0.001	0.227	166	0.080	0.006	0.592	640	0.025	0.001	0.237	319	0.056	0.003
Carrara Marble	0.312	81	0.031	0.003	0.146	81	0.072	0.008	0.328	44	0.048	0.007	0.159	54	0.065	0.009	0.310	155	0.020	0.002	0.175	80	0.161	0.018	0.314	280	0.030	0.002	0.151	135	0.079	0.006
Carrara Marble CIT																									0.326	21	0.027	0.006	0.144	24	0.081	0.017
CMTile					0.149	18	0.029	0.007	0.315	303	0.029	0.002	0.145	291	0.060	0.004	0.310	160	0.019	0.001	0.156	144	0.098	0.008	0.313	463	0.026	0.001	0.145	309	0.059	0.003
47407 Coral																									0.707	9	0.025	0.008	0.275	11	0.071	0.021
DH-2-10																									0.554	11	0.013	0.004	0.236	16	0.082	0.020
DH-2-11																									0.560	19	0.027	0.006	0.196	17	0.035	0.009
DH-2-12																									0.564	18	0.025	0.006	0.243	16	0.032	0.008
DH-2-13																									0.568	17	0.027	0.006	0.261	19	0.063	0.014
DH-2 Combined																									0.562	65	0.024	0.003	0.234	68	0.058	0.007
ETH-1	*0.207	85	0.025	0.003	*0.130	88	0.051	0.005	*0.205	402	0.026	0.001	*0.133	376	0.065	0.003	*0.206	284	0.020	0.001	*0.139	188	0.105	0.008	0.206	771	0.023	0.001	0.132	464	0.062	0.003
ETH-2	*0.208	69	0.020	0.002	*0.131	73	0.064	0.008	*0.206	386	0.027	0.001	*0.133	366	0.056	0.003	*0.207	271	0.024	0.001	*0.156	204	0.110	0.008	0.206	726	0.025	0.001	0.132	439	0.058	0.003
ETH-3	*0.612	69	0.023	0.003	*0.244	68	0.054	0.007	*0.602	184	0.027	0.002	*0.249	168	0.058	0.004	*0.614	210	0.022	0.002	*0.25	145	0.082	0.007	0.609	463	0.025	0.001	0.247	236	0.057	0.004
ETH-4	0.455	64	0.020	0.003	0.198	70	0.059	0.007	0.441	191	0.026	0.002	0.203	187	0.058	0.004	0.445	208	0.021	0.001	0.206	171	0.106	0.008	0.445	463	0.023	0.001	0.201	257	0.058	0.004
IAEA-C1									0.300	68	0.025	0.003	0.143	49	0.056	0.008	0.294	15	0.017	0.004	0.142	15	0.141	0.036	0.299	83	0.024	0.003	0.143	49	0.056	0.008
IAEA-C2									0.642	60	0.025	0.003	0.273	59	0.062	0.008	0.624	14	0.021	0.005	0.236	13	0.067	0.018	0.638	74	0.025	0.003	0.273	59	0.062	0.008
ISTB-1																									0.663	15	0.059	0.015	0.297	12	0.047	0.014
Mallinckrodt																	0.465	16	0.042	0.011	0.136	13	0.081	0.023	0.465	16	0.042	0.011				
Merck									0.514	67	0.030	0.004	0.234	59	0.055	0.007	0.514	14	0.030	0.008	0.175	11	0.170	0.051	0.514	81	0.030	0.003	0.234	59	0.055	0.007
NBS 19																	0.316	8	0.025	0.009	0.116	7	0.073	0.027	0.316	8	0.025	0.009				
SPEL-2-8-E																									0.596	11	0.035	0.011	0.245	11	0.089	0.027
SRM88B																	0.528	11	0.017	0.005	0.424	10	0.153	0.048	0.528	11	0.017	0.005				
TB-1																									0.327	21	0.034	0.007	0.133	23	0.089	0.019
TB-2																									0.335	19	0.035	0.008	0.164	19	0.095	0.022
TV01																									0.619	22	0.028	0.006	0.260	25	0.077	0.015
TV03	0.626	47	0.019	0.003	0.267	58	0.043	0.006									0.626	80	0.019	0.002	0.212	32	0.063	0.011	0.626	127	0.019	0.002	0.267	58	0.043	0.006
Veinstrom	0.636	102	0.026	0.003	0.272	100	0.066	0.007	*0.634	322	0.030	0.002	*0.274	336	0.059	0.003	0.632	304	0.023	0.001	0.252	193	0.079	0.006	0.633	728	0.026	0.001	0.273	436	0.061	0.003

Table 5. Theoretical equilibrium Δ_{63} and Δ_{64} for calcite (Hill et al., 2014; Tripati et al., 2015), acid fractionation factors (AFFs) $\Delta^*_{63\text{-}47}$ and $\Delta^*_{64\text{-}48}$ for the phosphoric acid digestion of calcite to CO_2, and calcite equilibrium Δ_{47} and Δ_{48} values. The AFFs were calculated using regressions determined from the difference in theoretical Δ_{63} and Δ_{64} values at 600 °C and 33.7 °C and samples with known precipitation temperatures, ETH-1 (600 °C), ETH-2 (600 °C), and Devils Hole calcite (33.7 °C). Δ_{47} and Δ_{48} values were calculated as $\Delta_{63} + \Delta^*_{63\text{-}47} = \Delta_{47\ \text{I-CDES}}$ and $\Delta_{64} + \Delta^*_{64\text{-}48} = \Delta_{48\ \text{CDES 90}}$, using equations 7 and 8, respectively.

Temperature	Δ_{63} (‰) (Hill et al., 2014; Tripati et al., 2015)	$\Delta^*_{63\text{-}47}$ (‰)	$\Delta_{47\ \text{I-CDES}}$ (‰)	Δ_{64} (‰) (Hill et al., 2014; Tripati et al., 2015)	$\Delta^*_{64\text{-}48}$ (‰)	$\Delta_{48\ \text{CDES 90}}$ (‰)
0	0.470	0.197	0.667	0.156	0.131	0.287
10	0.438	0.196	0.634	0.140	0.131	0.271
20	0.408	0.196	0.604	0.126	0.131	0.257
22	0.402	0.196	0.598	0.123	0.131	0.254
25	0.394	0.195	0.589	0.120	0.131	0.251
30	0.381	0.195	0.576	0.114	0.131	0.245
33.7 (DH-2)	0.371	0.195	0.566	0.109	0.131	0.240
40	0.355	0.195	0.550	0.103	0.131	0.233
50	0.332	0.194	0.526	0.093	0.131	0.224
60	0.310	0.194	0.504	0.084	0.131	0.215
70	0.290	0.193	0.483	0.076	0.131	0.207
80	0.271	0.193	0.464	0.069	0.131	0.200
90	0.254	0.193	0.446	0.063	0.131	0.194
100	0.238	0.192	0.430	0.058	0.130	0.188
200	0.128	0.190	0.318	0.025	0.130	0.155
300	0.073	0.189	0.262	0.012	0.130	0.142
400	0.044	0.189	0.232	0.006	0.130	0.136
500	0.027	0.188	0.216	0.004	0.130	0.134
600	0.018	0.188	0.206	0.002	0.130	0.132
700	0.012	0.188	0.200	0.002	0.130	0.132
800	0.009	0.188	0.197	0.001	0.130	0.131
900	0.006	0.188	0.194	0.001	0.130	0.131
1000	0.005	0.188	0.192	0.001	0.130	0.131

Table 6. Δ_{47} and Δ_{48} data for Devils Hole cave calcite from this study, Bajnai et al. (2021), and Fiebig et al. (2021).

	Sample	Age (ka)	N	$\Delta_{47\ I\text{-}CDES}$ (‰)	$\Delta_{47\ CDES\ 90}$ (‰)	Δ_{47} SE	N	$\Delta_{48\ CDES\ 90}$ (‰)	Δ_{48} SE
This study	DH-2-10	168-176	11	0.554		0.004	16	0.236	0.020
	DH-2-11	159-167	19	0.560		0.006	17	0.196	0.009
	DH-2-12	152-162	18	0.564		0.006	16	0.243	0.008
	DH-2-13	146-156	17	0.568		0.006	19	0.261	0.014
	Average		65	0.562		0.003	68	0.234	0.007
Bajnai et al., 2021	DHC2-8	4.5-16.9	14		0.573	0.002	9	0.255	0.009
	DHC2-3	32.2-39.8	9		0.575	0.003	N is the same as for Δ_{47}	0.252	0.009
	DH-11 19.7	86.4-94.3	9		0.572	0.001		0.255	0.009
	DH-11 44.5	121.8-123.7	12		0.581	0.002		0.226	0.008
	DH-11 73.0	176.1-184.8	9		0.575	0.002		0.250	0.008
	DH-11 109.4	232.8-240.5	23		0.575	0.001		0.227	0.006
	DH-11 141.6	291.3-299.0	9		0.570	0.002		0.223	0.009
	DH-11 189.9	353.0-358.3	14		0.574	0.002		0.232	0.006
	DH-11 201.3	371.7-388.4	9		0.568	0.002		0.250	0.010
	DH-11 296.6	485.5-507.8	8		0.575	0.002		0.243	0.008
	Average		116		0.574	0.003	111	0.239	0.003
Fiebig et al., 2021	DVH-2	4.5-16.9	9	0.582		0.003	N is the same as for Δ_{47}	0.246	0.012
	DHC2-8	4.5-16.9	8	0.585		0.006		0.234	0.013
	DHC2-8	4.5-16.9	9	0.572		0.003		0.234	0.012
	DHC2-8	4.5-16.9	5	0.576		0.004		0.247	0.016
	Average		31	0.580		0.002	31	0.237	0.008
Combined average	Average		212	0.571		0.001	210	0.238	0.007